Author/s:
Morrongiello, JR;Horn, PL;Ó Maolagáin, C;Sutton, PJH

Title:
Synergistic effects of harvest and climate drive synchronous somatic growth within key New Zealand fisheries

Date:
2021-04-01

Citation:
Morrongiello, J. R., Horn, P. L., Ó Maolagáin, C. & Sutton, P. J. H. (2021). Synergistic effects of harvest and climate drive synchronous somatic growth within key New Zealand fisheries. Global Change Biology, 27 (7), pp.1470-1484. https://doi.org/10.1111/gcb.15490.

DR. JOHN MORRONGIELLO (Orcid ID : 0000-0002-9608-4151)

Article type   : Primary Research Articles

Synergistic effects of harvest and climate drive synchronous somatic growth within key New Zealand fisheries

Running head: Fishing and climate drive growth synchrony

J.R. Morrongiello[1], P.L. Horn[2], C. Ó Maolagáin[2], P.J.H. Sutton[2]

[1] School of BioSciences, University of Melbourne, Victoria, Australia

[2] National Institute of Water and Atmospheric Research (NIWA), New Zealand

Corresponding author:

John Morrongiello, School of BioSciences, University of Melbourne, +61 3 8344 8929, john.morrongiello@unimelb.edu.au

Abstract

Fisheries harvest has pervasive impacts on wild fish populations, including the truncation of size and age structures, altered population dynamics and density, and modified habitat and assemblage composition. Understanding the degree to which harvest-induced impacts increase the sensitivity of individuals, populations and ultimately species to environmental change is essential to ensuring sustainable fisheries management in a rapidly changing world. Here, we generated multiple long-term (44 to 62 years), annually resolved, somatic growth chronologies of four commercially important fishes from New Zealand's coastal and shelf waters. We used these novel data to investigate how regional- and basin-scale environmental variability, in concert with fishing activity, affected individual somatic growth rates and the magnitude of spatial synchrony among stocks. Changes in somatic growth can affect individual fitness and a range of population and fishery metrics such as recruitment success, maturation schedules and stock biomass. Across all species, individual growth benefited from a fishing-induced release of density controls. For nearshore snapper and tarakihi, regional-scale wind and temperature also additively affected growth, indicating that future climate change-induced warming and potentially strengthened winds will initially promote the productivity of more poleward populations. Fishing increased the sensitivity of deep-water hoki and ling growth to the Interdecadal Pacific Oscillation (IPO). A forecast shift to a positive IPO phase, in concert with current harvest strategies, will likely promote individual hoki and ling growth. At the species level, historical fishing practices and IPO synergised to strengthen spatial synchrony in average growth between stocks separated by 400-600 nm of ocean. Increased spatial synchrony can, however, increase the vulnerability of stocks to deleterious stochastic events. Together, our individual- and species-level results show how fishing and environmental factors can conflate to initially promote individual growth but then possibly heighten the sensitivity of stocks to environmental change.

Keywords

Spatial synchrony; otolith biochronology; climate change; dispersal; fishing; Pacific Ocean; Moran Effect; population dynamics; density-dependent growth

Introduction

The degree to which life history parameters are spatially synchronous plays a critical role in determining the abundance and persistence of wild populations, as greater levels of synchrony increase the likelihood that all populations in a region will express good or poor performance simultaneously (Liebhold *et al.*, 2004, Schindler *et al.*, 2010). Spatial synchrony is a common feature of wild populations, with its magnitude and extent dependent on rates of individual dispersal, strength of environmental factors ('Moran Effect'), or the widespread influence of interspecific trophic interactions (reviewed by Liebhold *et al.*, 2004). Importantly, anthropogenic stress, such as that induced by fisheries harvest, can also drive an increase in spatial synchrony (Frank *et al.*, 2016), as age and size truncation decrease demographic buffering and in turn increase instability in population dynamics (Anderson *et al.*, 2008, Gamelon *et al.*, 2019, Rouyer *et al.*, 2012). Understanding the causes and consequences of spatiotemporal population dynamics greatly enhances our capacity to predict and manage natural systems and natural resource yields in the face of rapid anthropogenic environmental change (Engen *et al.*, 2018, Rouyer *et al.*, 2012, Schindler *et al.*, 2010).

Sustainable management of wild fisheries relies on sound understanding of how individual fish, and the populations they comprise, respond to harvest and stochastic or directional environmental forcing such as ocean warming (Audzijonyte *et al.*, 2016, Kjesbu *et al.*, 2014, Le Bris *et al.*, 2018). Historically, the impacts of fishing and environmental fluctuations on population dynamics have been considered in isolation. Harvest is seen as exploitative and affects population averages, whereas climate fluctuations affect population variance (reviewed by Planque *et al.*, 2010). Potential synergies between the two have only come into focus more recently. For example, increased adult mortality due to fishing can decrease recruitment strength and thus increase the sensitivity of recruitment success to environmental variation (Rouyer *et al.*, 2011). Similarly, harvest can select on reproductive phenology and drive potential mismatches between spawning windows and favourable environmental conditions (Rogers & Dougherty, 2019), or constrain the expression of thermally-dependent growth phenotypes through alterations to social hierarchies or density (Morrongiello *et al.*, 2019). Habitat loss and degradation due to fishing activity can reduce carrying capacities and also increase the sensitivity of populations to additional environmental change (Brown *et al.*, 2019). Conversely, fishing-induced reductions in density (Lorenzen & Enberg, 2002) can facilitate fish survival in potentially sub-optimal warmer waters (Ciannelli *et al.*, 2004). Importantly here, both warming (Morrongiello & Thresher, 2015) and harvest (Schindler *et al.*, 2010) are known to induce spatial synchrony in fish populations. Increased synchrony can heighten the vulnerability of individual stocks to deleterious stochastic events as struggling populations will fail to receive demographic rescue from more successful populations (Heino *et al.*, 1997), and could even promote species-wide fishery collapse (Lobón-Cerviá, 2009).

The World's oceans have experienced recent rapid warming (Cheng *et al.*, 2019) and prolonged fisheries exploitation (Hilborn *et al.*, 2020). These changes have occurred against a backdrop of large and small-scale natural environmental variations that affect individual fitness and population dynamics. For example, El Niño/Southern Oscillation (ENSO) and the Interdecadal Pacific Oscillation (IPO) are basin-wide climate and oceanographic signals and have been implicated in ecosystem regime shifts (e.g. Hare & Mantua, 2000). On a more regional scale, interannual variation in zonal wind strength affects fish recruitment patterns (Jenkins, 2005) whilst the magnitude of upwelling can influence fish growth (Black *et al.*, 2011). It is essential to understand how regional and basin-scale anthropogenically and naturally driven environmental variations interact with fishing activity to influence patterns of spatial synchrony. In turn, this understanding informs the adaptation of fisheries management and fisher behaviour to ensure fisheries viability in the future (Audzijonyte *et al.*, 2016, Perry *et al.*, 2010, Planque *et al.*, 2010).

Somatic growth rate describes how an individual's size-at-age changes through time and is highly sensitive to a range of intrinsic (within individual), natural and anthropogenic extrinsic factors (Enberg *et al.*, 2012, Morrongiello & Thresher, 2015). Growth is an ideal candidate with which to explore the impacts of fishing and environmental variability because it not only underpins individual fitness (e.g., size-dependent survival and reproduction, Barneche *et al.*, 2018, Sogard, 1997), but also a range of population-level metrics such as recruitment success (Bergenius *et al.*, 2002), maturity schedules (Uusi-Heikkilä *et al.*, 2015), and stock biomass (Stawitz & Essington, 2019). Growth rate is dependent on the amount of acquired resources and subsequent allocation trade-offs among maintenance and reproduction (Enberg *et al.*, 2012). Environmental- and fishing-induced changes to resource availability and competition can thus affect the expression of growth (Morrongiello *et al.*, 2019). Likewise, size selective harvest and increased mortality can select for earlier age at maturation and an associated increase in juvenile growth rate (Uusi-Heikkilä *et al.*, 2015), whilst temperature-dependent metabolic costs can limit energy available to be allocated towards growth (Neuheimer *et al.*, 2011). Therefore, whilst it is intuitive to think of elevated growth rate as being 'good' for an individual, it is important to acknowledge that it can also be symptomatic of a population under stress (Trippel, 1995). The growth information naturally archived in fish otoliths offers an opportunity to identify and quantify the drivers of individual growth variation within wild populations (Morrongiello *et al.*, 2012) and spatial synchrony at the species and assemblage level (Martino *et al.*, 2019, Ong *et al.*, 2018, Tanner *et al.*, 2020).

The waters around New Zealand support significant commercial fisheries on both inshore and deep-water species (Fisheries New Zealand, 2019) and have undergone warming associated with climate change (Sutton & Bowen, 2019). Here, we use the unique biological information naturally archived in fish otoliths collected during routine fisheries assessments to recreate 44- to 62-year-long biochronologies of average annual fish growth for four commercially important fishes. We then relate these estimates of inter-annual growth variability to environmental changes that are manifest on both basin- and regional spatial scales. We adopt a hierarchy of analyses to sequentially ask: 1) do environmental and fishing variables additively or synergistically affect the expression of individual growth within species; 2) what is the level of spatial synchrony in growth within and among focal species; and 3) how does basin and regional-scale environmental variability and fishing pressure affect the magnitude and direction of spatial synchrony? We predict that individual fish growth will become more sensitive to environmental drivers during periods of elevated fishing pressure. Furthermore, spatial synchrony will be greatest within species across areas, followed by between species in the same area and then between species across areas. These synchrony patterns arise because of implicit similarities and differences in environmental and fishing responses within and among species respectively, and potential dispersal between stocks linking population dynamics. By simultaneously assessing how environmental variability and fishing pressure affect individuals, populations and species, we can develop a holistic understanding of the impact of these changes and in turn make more meaningful predictions of future fishery productivity.

Methods

Study species and system

We developed growth biochronologies for two inshore and two deep-water New Zealand fishes. Snapper (*Chrysophrys auratus*) and tarakihi (*Nemadactylus macropterus*) are demersal inshore species occurring in water depths from 5 to 250 m (Anderson *et al.*, 1998). Both species have been sampled regularly since the 1980s from the northeast of North Island's Hauraki Gulf and East Cape region (snapper: HAGU; tarakihi: NENI), and off northern South Island primarily in Tasman Bay and the west coast (snapper: TBGB; tarakihi: TBWC, Figure 1a). Tagging data and analyses of growth rates and year class strengths indicate that both species comprise separate stocks in each sampled area (Fisheries New Zealand, 2019),with tarakihi tending to move more than snapper.

Hoki (*Macruronus novaezelandiae*) and ling (*Genypterus blacodes*) are predominantly deep-water demersal species abundant around South Island in depths from 200 to 800 m (Anderson *et al.*, 1998). Trawl surveys monitoring these species have been conducted regularly since the 1980s on Chatham Rise and the Campbell Plateau (Figure 1a). Hoki comprise two stocks, one having a home ground on the Campbell Plateau (CAMP) and a spawning ground off the west coast of South Island, and the other spawning in Cook Strait and having a home ground on Chatham Rise (CHAT; Livingston *et al.*, 2015). Ling on Chatham Rise (CHAT) are clearly distinct from Campbell Plateau (CAMP) fish because of marked between-area differences in growth rates and year class strengths (Horn, 2005). All eight nearshore and deep-water stocks are assessed and managed separately (Fisheries New Zealand, 2019). See Table S1 for additional biological and management details.

Otolith samples

For each area-species combination, we followed the sampling design of Morrongiello et al. (2012) and selected otoliths based on their year of collection and previously estimated age. This approach ensured good coverage of year classes (3-78 fish per collection, x̄=28.7), replication of fish ages throughout the reconstructed growth time series, and 3681-5330 increment measurements from 435-521 fish per area (Figure 1b; Table 1). All otoliths were re-aged following validated otolith interpretation protocols (Horn & Sutton, 2017, Horn, 1993, Walsh *et al.*, 2016, Walsh *et al.*, 2014). We sampled snapper aged 3–20 years, tarakihi aged 2–26, hoki aged 4–15, and ling aged 4–19 (i.e., if possible avoiding the oldest fish which were likely to have very narrow, and hence, less informative growth zones near the otolith margin). It was necessary, however, to sample 2–10% of fish from older ages to enable the planned coverage of year classes across sample years. We aimed to sample 9–10 fish from each species-area year class, with even proportions by sex.

Annual growth increments were measured from images of sagittal otolith cross-sections (Figure 1c) in ImageJ (Abràmoff *et al.*, 2004). Our approach assumes that otolith increments are a proxy of fish growth. We tested and confirmed this assumption for all species by regressing fish length on otolith radius (snapper $R^2 = 0.705$, $n = 938$; tarakihi: $R^2 = 0.643$, $n = 985$; hoki: $R^2 = 0.429$, $n = 1005$; ling: $R^2 = 0.830$, $n = 1012$).

Fishery and environmental predictors

For each of the eight species-area combinations, we developed a series of environmental and fishery-related predictor variables (defined in Table 2; Figure S1). Environmental predictor series were derived for the basin-scale Southern Oscillation Index (*SOI*) and inter-decadal Pacific Oscillation Index (*IPO*), and the regional scale sea surface temperature (*SST*), Trenberth indices of wind direction and strength *(Z & M*), and offshore *wind stress* magnitude. Temperature-at depth data (e.g. Simple Ocean Data Assimilation [SODA3] reanalysis: Carton *et al.*, 2018) was not available for the full study period and therefore we used *SST* to describe the benthic thermal regime inhabited by our focal species. This is justified for nearshore species as the maximum mixed layer depth in New Zealand waters is 250 m (Bowen *et al.*, 2017), which encompasses the modal depth of catch for snapper and tarakihi (~20 m and ~150 m respectfully; Anderson *et al.*, 1998, Fisheries New Zealand, 2019). SST variation around New Zealand has also been linked to water temperatures down to 800 m (Bowen *et al.*, 2017, Sutton *et al.*, 2005) which encompasses the environment of our deep-water species (modal catch for hoki ~ 550 m and ling ~ 500 m; Anderson *et al.*, 1998, Fisheries New Zealand, 2019). Series of spawning stock biomass (*SSB*) and fishing pressure (*FP*; catch/biomass vulnerable to fishing) were derived from stock assessments (Fisheries New Zealand, 2019).

The environmental series were constructed in line with each species' 'growth year', i.e., the year beginning at the fish's birthday. For both hoki and ling, the growth year is September to the following August. For snapper, the growth year was from January to the following December and for tarakihi April to the following March. For each available series, an annual index was developed (e.g., for ling: mean *SST* for the September–August year), as well as four three-monthly indices (e.g., for ling: September–November, December–February, March–May, June–August). We also estimated environmental conditions in the year preceding fish growth to explore potential lagged effects, necessary when examining linkages between the higher-order consumer production observed here and environmental factors that may operate through trophic pathways (Nguyen *et al.*, 2015).

Statistical analyses

Variation in annual growth increments were analysed using mixed effects modelling (Morrongiello & Thresher, 2015). A random intercept for each *Fish* induces a correlation among increments to account for any individual-specific differences in growth and the repeated measures nature of otolith increment data. A random intercept for A*rea:year* (unique identifier for each growth year within an area) induces a correlation among increments from different fish living in the same are that were deposited in the same year, and accounts for potential temporal growth differences induced by common environmental effects. Otolith increment width exponentially declines with fish age and this pattern is generally linearised by taking the natural log of both variables. However, a preliminary exploration of model residuals indicated that such an approach did not fully describe the growth-age relationship for the four species. Therefore, we explored whether the inclusion of a quadratic for log-transformed age improved model fit. Mixed effects models were developed using the ‘lme4’ package (Bates *et al.*, 2015) in R 3.5.1.

Intrinsic drivers of annual growth and biochronology development

We developed a series of base growth models for each species that included three-way interactions between *Age* (linear or quadratic) and *Area* and *Sex*. These terms allowed for spatial and sex-specific differences in the average growth-age relationship. We also included an interaction between *age-at-capture* (*AAC*) and *Area* to account for potential biases in estimated growth rates associated with differential mortality or sampling regime at each area (see Morrongiello *et al.*, 2012 for discussion). *Age* and *age-at-capture* were scaled $[(x-\overline{x})/s]$ to facilitate model convergence and interpretation of interactions and quadratic terms. Base models included random intercepts for *Fish* and *Area:year* and their associated random *Age* (linear and quadratic) slopes. These complex random slope structures allow for individual-specific and year -specific deviations from the average growth-age relationship. The most complex base intrinsic effects model can be represented by:

$$\begin{gathered} y_{ijklmn} = \alpha_k + \alpha_{Yk,l} + \alpha_{Fi} + \beta_A x_{j(k,m)} + \beta_A^2 x_{j(k,m)} + \gamma_C z_n a_k + b_{FA} x_{ij} + b_{YA} x_{j(k),l} + \varepsilon_{ijk} \\ \begin{bmatrix} \alpha_{Fi} \\ b_{FAi} \end{bmatrix} N(0,\textstyle\sum_i),\begin{bmatrix} a_{Yk,l} \\ b_{YAk,l} \end{bmatrix} N(0,\textstyle\sum_{k,l}),\varepsilon_{ijk}\, N(0,\sigma^2) \end{gathered}$$

(Eq. 1)

where y_{ijkmn} is the annual otolith increment (µm) for the ith fish at age j from area k in year l and sex m that is caught at age n, α_k is the fixed (area-specific average) annual growth intercept, $\alpha_{Yk,l}$ is the random extrinsic effect for *Area* k at *growth year* l, α_{Fi} is the random intrinsic fish effect, $\beta_{Aj(k,m)}$ and $\beta^2_{Aj(k,m)}$describe the linear and quadratic components of age-dependent change in growth specific to each *Area* k and *Sex* m, $\gamma_{Cn(k)}$ is the interaction between *age-at-capture* z and *Area* k, b_{FAij} is the random slope of *Age* for fish i, $b_{YAjk,l}$ is the random slope of *Age* for *Area* k at *growth year* l and ε is assumed to be independent errors with mean zero and common variance σ^2.

We compared the performance of eight random effects structures that included different combinations of linear and quadratic *Age* random slopes for *Fish* and *Area:year*. These models were forced to include the maximal intrinsic effects structure (*Age * Area * Sex +*

Age^2 ** Area * Sex* + *age-at-capture * Area*), were fit with restricted maximum likelihood (REML), and compared using Akaike's Information Criterion corrected for small sample sizes (AIC$_c$). We then applied each species' best random effects structure to models with increasing fixed intrinsic effect complexity, fit with maximum likelihood (ML), and compared these with AICc. The best intrinsic model for each species was reanalysed using REML to produce unbiased parameter estimates.

Extrinsic drivers of annual growth: basin-wide versus regional scale

The impact of fishery activity, demography and environmental variation on each species' annual growth was assessed by including additional extrinsic variables to the best intrinsic model structure for each species (from Eq. 1). *SST, Wind Stress, SSB* and *FP* were scaled $\left[(x_{ijk} - \dot{x}_{jk})/s_{jk}\right]$ within each area (*j*) and species (*k*). *IPO, SOI* and *Trenberth M* and *Z* values were the same across areas for a species and so were just scaled $\left[(x_{ik} - \dot{x}_{k})/s_{k}\right]$ within each species (*k*). We included an interaction term with *Area* for all scaled variables so that growth responses could be conditional on location. We built and compared two broad suites of models: those that included basin-scale environmental drivers (*IPO* or *SOI*, which both affect *SST* and winds) and those that included more regionalised environmental drivers (*SST*, wind indices). We allowed *SSB* and *FP* to be included in both model sets and tested for interactions between these fishing variables and basin-wide and regional environmental drivers. *IPO* and *SOI* both describe large-scale environmental processes, and *Trenberth M* and *Z* and *Wind Stress* (offshore) all describe wind-related phenomena. *SSB* and *FP* are related to fishing activity. Competing models therefore included either *IPO* and *SOI*, either of the three wind variables, and either of the two fishing activity series to allow for meaningful comparisons of their relative importance. We included just linear terms for each extrinsic variable to manage model complexity. Competing environmental models were fit with ML and compared using AICc. The best environmental model for each species was then refit with REML. Parameter estimates and 95% credible intervals were derived from the posterior distribution of the fixed effects in the best model using 1000 model simulations generated by the 'arm' package (Gelman & Su, 2020), and model predictions generated using the 'effects' package (Fox & Weisberg, 2019).

Spatial synchrony in annual growth

We extracted the *Area.year* random effect conditional modes (best linear unbiased predictors, BLUPs) from each species' best base intrinsic effects model (model not including fixed extrinsic variables) and used these biochronologies to explore spatial synchrony in growth within and among species (sensu Tanner *et al.*, 2020). Temporal trends were removed from each biochronology using a first-order autoregressive model that included a linear term for year and the resultant residuals taken forward for further analysis (Buonaccorsi *et al.*, 2001). Zero-lag cross correlations were performed between each residual growth series to estimate overall levels of spatial synchrony. Then, we calculated 21-year centre-aligned running correlations (using the 'running' function from the 'gtools' package in R: Warnes *et al.*, 2020) between the residual growth series within each species to explore temporal patterns in spatial synchrony. A span of 21 years was selected as a compromise between correlation robustness (maximised by greater span) and the need to identify shorter-term changes in synchrony (maximised by shorter span). Running correlation significance at the 0.05 level was assessed by taking 1000 Monte Carlo simulations of 21-year running correlations based on randomly generated data of the same length as that of each growth time series. We extracted the highest running correlation for each simulation and used the resulting distribution to identify the critical threshold of running correlations above which they are significant at p=0.05. Repeatedly testing the significance of each running correlation without simulation would greatly inflate Type 1 error rates due to multiple comparisons.

Where necessary, we scaled and then took time-dependent averages of predictor variables that differed between areas for a species (*SSB, FP, SST, wind stress*) to generate a single series. We then calculated 21-year centre-aligned rolling means (using the 'rollmean' function from the 'zoo' package in R) for each annually derived fishery and environmental variable to match the growth running correlation data described above. We explored how these time-averaged annual predictor variables influenced the degree of within-species spatial synchrony using a first order autoregressive model that accounted for temporal autocorrelation. Each environmental variable was interacted with fishing variables and competing models, along with the null which included just a model intercept, were compared using AICc.

Results

Intrinsic drivers of growth

The best supported random effects structure for all species included random linear and quadratic age slopes for *Fish* (Table S2), indicating that the growth-age relationship varied among individual fish. Snapper and ling models also included random linear and quadratic age slopes for *Area:year* (Table S2), indicating that there were differences in age-dependent growth across years. There was some variation in the composition of the best intrinsic effects model among species (Table S3). For all species, growth declined with age and varied across regions (Table 3; Figure 2). Sex-dependent differences were only evident for ling, where females consistently grew faster than males from about 7 years of age (Table 3; Figure 3). Age-dependent biases in estimated growth rates were detected, and accounted for, in all species using the *age-at-capture* term. Specifically, snapper and tarakihi caught at older ages consistently grew slower than fish caught when younger, whereas ling displayed the opposite pattern with fish caught at older ages being the faster growers (Table 3). The strength of these patterns differed between regions for snapper and ling.

Extrinsic drivers of annual growth: basin-wide versus regional scale

The growth of all four species was best explained by combinations of environmental factors and fishing activity calculated over either the winter-spring or lagged annual time periods (Table S4). Nearshore (snapper and tarakihi) and deep-water (hoki and ling) species systematically differed in the importance of regional versus basin-wide environmental drivers, and the synergistic impacts of fishing and the environment, on growth variation.

Snapper growth increased at a rate of 2.5%.$^{o}C^{-1}$ following warmer years (Figure 4a) and decreased at higher spawning stock biomasses (Figure 4b). There was a regional difference in how snapper responded to the previous years' *Trenberth Z1*, with a negative response in TBGB compared to a negligible response in HAGU (Figure 4c). The strength, but not direction, of the tarakihi growth response to *SST* during July-September differed among areas, with the poleward TBWC stock responding more positively (1.7%.$^{o}C^{-1}$) than the more equatorial NENI stock (0.6%.$^{o}C^{-1}$) (Figure 4d). Tarakihi grew faster in years with higher fishing pressure (Figure 4e) and windier winters (Figure 4f).

CHAT hoki growth was negligibly affected by the previous year's spawning stock biomass (**Figure 5**a). The growth of CAMP hoki was, however, much more sensitive to *SSB* with a steep decline in growth in years following large stock sizes (**Figure 5**a). We detected evidence for a synergistic impact of fishing and *IPO* on hoki growth (**Figure 5**b). At low spawning stock biomass, growth was positively related to the previous year's *IPO* index. At median biomass there was negligible effect of *IPO*, whereas at high biomass fish grew slower in years following those with more positive *IPO* indices.

CHAT ling growth was lower in years following large spawning stock biomass (**Figure 5**c). In contrast, *SSB* had a negligible impact on CAMP ling growth. Like hoki, we detected synergistic impacts of fishing and *IPO* on ling growth. Ling growth was positively related to *IPO* at low biomass, but negatively related to *IPO* at high biomass (**Figure 5**d).

Spatial synchrony in annual growth

HAGU and TBGB snapper experienced elevated growth during the mid-1980s, mid- to late-1990s, and mid- to late-2000s, and depressed growth during the mid- to late-1960s and 1992–1994 (Figure 6a). TBWC tarakihi displayed considerable interannual growth variation, with a period of pronounced growth depression from 1992–1996 which was followed by a period of elevated growth from 2000–2002 (Figure 6b). There was little evidence for strong consistent inter-annual growth variability synchrony among individuals in NENI tarakihi. Annual growth of CAMP and CHAT hoki increased in the decade following an early 1980s low point, and again for five years from a low point in the early 2000s (Figure 6c). Ling growth steadily declined for over a decade from 1980, and then remained depressed from 1993 onwards (Figure 6d). We detected no evidence for temporal trends in either snapper or tarakihi growth (area-specific OLS regressions, $p > 0.242$). Hoki CHAT growth increased by 6.5%.decade^{-1} ($p = 0.002$), whilst ling CAMP and ling CHAT decreased by 4.5%.decade^{-1} ($p < 0.001$) and 4%.decade^{-1} ($p < 0.001$) respectively.

Overall, fish growth rates were temporally synchronous across areas within species for snapper, hoki and ling (r(raw): 0.395–0.694, $p \leq 0.009$) and these patterns persisted after accounting for temporal trends and autocorrelation (r(res): 0.375-0.698, $p \leq 0.013$, Figure 6a,c,d). We identified consistent habitat-specific differences in the pattern of 21-year residual growth synchrony through time. Spatial synchrony in nearshore snapper and tarakihi residual growth time series steadily increased through time (Figure 6e-f). Conversely, spatial synchrony in the deep-water hoki and ling initially increased to a peak in the mid to late 1980 and early 1990s, then steadily declined to the early 2000s with some evidence for a recent increase in synchrony thereafter (Figure 6g-h). The best model explaining each species' temporal variation in spatial synchrony included *IPO*, and in three species *SSB* or *FP* (Table 4). Snapper spatial synchrony was highest in 21-year periods characterised by low *SSB* and a negative *IPO* phase (**Figure 7**a-b). Tarakihi spatial synchrony was best explained by an interaction between *IPO* and *FP* whereby correlations were strongest during periods of high fishing pressure and negative *IPO* (**Figure 7**c). Temporal variation in hoki synchrony was primarily related to positive *IPO* conditions (**Figure 7**d), and ling growth synchrony became more sensitive to *IPO* at higher *SSB* (**Figure 7**e). Between species, the only significant correlation in growth time series was between CAMP hoki and CHAT ling growth (r(res): 0.350, p = 0.022). There was little other evidence for strong growth synchrony among species.

Table 1: Summary of otolith sample data used to generate each growth biochronologies.

	Snapper		**Tarakihi**		**Hoki**		**Ling**	
	HAGU	**TBGB**	**NENI**	**TBWC**	**CHAT**	**CAMP**	**CHAT**	**CAMP**
Number of individuals	446	447	521	435	482	499	504	507
Number of increments	4020	4837	4431	4492	3681	4063	5330	5240
Growth biochronology span	1954-2013 (60 years)	1960-2014 (55 years)	1954-2015 (62 years)	1962-2016 (55 years)	1972-2015 (44 years)	1973-2016 (44 years)	1965-2015 (51 years)	1968-2016 (49 years)

Table 2: Description of environmental and fishing-related predictor variables used in spatial synchrony and annual growth models for four species of New Zealand fish.

Variable type	**Variable**	**Description**	**Available time span**
Basin-wide environment	Southern Oscillation Index (SOI)	Difference in surface atmospheric pressure between Tahiti and Darwin; a diagnostic Trade Wind strength and the El Niño/Southern Oscillation (ENSO) system. El Niño's are normally associated with increased westerly and southerly winds (Salinger *et al.*, 1995) and cooler ocean temperatures around New Zealand (Sutton & Roemmich, 2001).	1950-2016
	Interdecadal Pacific Oscillation (IPO)	A filtered tripole index from Henley et al. (2015). Cooler ocean and stronger south-westerly wind conditions around New Zealand in positive IPO phases (Hannah & Bell, 2012).	1950-2016
Regional environment	Sea surface temperature (SST)	Two *SST* products are used in this analysis: 1) reconstructed SST (NOAA Extended Reconstructed Sea Surface Temperature: ERSST.v5; available via http://www.esrl.noaa.gov/psd/) with a 2° latitude and longitude spatial resolution and monthly temporal resolution extending back to 1854 (Huang *et al.*, 2017); 2) objectively-analysed SST based on satellite measurement (NOAA OI	1960-2016

		SST V2 High Resolution Dataset). The latter data are higher resolution (0.25° latitude and longitude spatial and daily temporal resolution) but are only available for the period since September 1981 (Reynolds *et al.*, 2007). SST series for each stock were developed for areas bounded by boxes in Figure 1a.	
	Trenberth (Z & M)	Changes in large-scale wind fields measured as normalised differences in mean sea level air pressure between points (Trenberth, 1976). By geostrophic balance, the pressure difference between two points is a direct proxy for the average strength of the surface wind perpendicular to that pressure difference. ‘Z’ indices describe zonal (westerly) winds and ‘M’ indices describe Meridional (northerly) winds. The indices and the pairs of geographical points defining them were for snapper and tarakihi: Z1 (Auckland – Christchurch) and M1 (Hobart – Chatham Islands); for hoki and ling: Z2 (Christchurch – Campbell Island) and M2 (Hokitika – Chatham Islands).	1950-2016
	Wind stress (offshore)	Mean offshore *wind stress* (i.e., the shear stress exerted by the wind on the surface of large bodies of water) in the areas of interest extracted from the JRA-55 reanalysis (http://jra.kishou.go.jp/JRA-55/index_en.html) (Kobayashi *et al.*, 2015). Related to regional changes in wind forcing and thus regional upper-ocean circulation and mixing.	1960-2016
Fishing	Spawning stock biomass (SSB)	Combined weight of all individuals in a stock that have reached sexual maturity (tonnes). Measure of adult population abundance and, assuming relatively stable distribution, density-dependent competition. Data from Fisheries New Zealand (2019).	Snapper: 1950-2015 Tarakihi: 1950-2017 Hoki: 1972-2016 Ling: 1971-2016
	Fishing pressure (FP)	Annual catch/ biomass vulnerable to fishing. Measure of fishing intensity and selectivity. Data from Fisheries New Zealand (2019).	

Table 3: Fixed effect parameter estimates (±95% confidence intervals) and random effect variance components for best intrinsic models explaining annual growth variation in four New Zealand fishes.

	Snapper			**tarakihi**			**hoki**			**ling**		
Fixed effects	**estimate (95% CI)**			**estimate (95% CI)**			**estimate (95% CI)**			**estimate (95% CI)**		
Intercept	4.284 (4.263, 4.305)			3.812 (3.795, 3.829)			4.439 (4.421, 4.458)			5.804 (5.784, 5.824)		
Age	-0.426 (-0.440, -0.413)			-0.493 (-0.506, -0.480)			-0.479 (-0.490, -0.467)			-0.592 (-0.612, -0.573)		
Age^2	0.156 (0.148, 0.166)			0.019 (0.012, 0.025)			0.069 (0.060, 0.078)			-0.151 (-0.168, -0.135)		
Age-at-capture	-0.051 (-0.066, -0.035)			-0.021 (-0.030, -0.011)			–			0.016 (0.006, 0.026)		
Area	0.205 (0.178, 0.233)			-0.023 (-0.044, -0.001)			0.032 (0.005, 0.057)			-0.096 (-0.121, -0.068)		
Sex	–			–			–			0.049 (0.024, 0.075)		
Age * Area	-0.075 (-0.094, -0.055)			-0.039 (-0.053, -0.025)			-0.020 (-0.036, -0.005)			-0.173 (-0.200, -0.150)		
Age^2 * Area	-0.087 (-0.099, -0.074)			–			-0.011 (-0.023, 0.002)			-0.029 (-0.050, -0.009)		
Age * Sex	–			–			–			0.066 (0.044, 0.086)		
Age^2 * Sex	–			–			–			0.032 (0.017, 0.048)		
Area * Sex	–			–			–			-0.024 (-0.050, 0.004)		
Age-at-capture * Area	0.031 (0.011, 0.049)			–			–			-0.008 (-0.021, 0.006)		
Random effects	**σ**	**corr**		**σ**	**corr**		**σ**	**corr**		**σ**	**corr**	
Fish	0.127			0.149			0.156			0.140		
Age|Fish	0.075	0.06		0.104	0.09		0.079	0.19		0.120	0.28	
Age^2|Fish	0.049	-0.59	0.42	0.061	-0.49	0.63	0.054	-0.71	0.53	0.091	-0.68	0.43
Area:year	0.047			0.017			0.022			0.020		
Age|Area:year	0.020	-0.19								0.030	-0.90	

Age^2 | Area:year	0.012	-0.60	-0.11							0.032	-0.99	0.86
Residual	0.129			0.136			0.192			0.218		

Table 4: Results of environmentally driven spatial synchrony model selection for four New Zealand fishes. Shown are the top three models (based on AICc) for each species. The best supported model for each species has a ΔAICc of 0 and is highlighted in bold. df = degrees of freedom.

Species and model	**df**	**Log likelihood**	**AICc**	**ΔAICc**
Snapper				
IPO_{ann} + SSB_{ann}	**5**	**52.659**	**-93**	**0**
SSB_{ann}	4	51.008	-92.5	0.48
SSB_{ann} + $TrenZ1_{ann}$	5	52.336	-92.4	0.65
Intercept only	**3**	**46.694**	**-86.5**	**6.5**
Tarakihi				
IPO_{ann}	**4**	**36.993**	**-63.8**	**0**
IPO_{ann} * SSB_{ann}	6	40.446	-63.6	0.12
IPO_{ann} * FP_{ann}	6	39.666	-62.1	1.68
Intercept only	3	30.632	-54.3	9.5
Hoki				
FP_{ann}	**4**	**36.993**	**-63.8**	**0**
IPO_{ann} * SSB_{ann}	6	40.446	-63.6	0.12
IPO_{ann} * FP_{ann}	6	39.666	-62.1	1.68
Intercept only	3	32.002	-56.7	7.0
Ling				
IPO_{ann} * SSB_{ann}	**6**	**44.881**	**-72.5**	**0**
IPO_{ann} * FP_{ann}	6	42.447	-67.6	4.87
SOI_{ann} * FP_{ann}	6	36.923	-56.6	15.92
Intercept only	3	28.998	-50.7	21.8

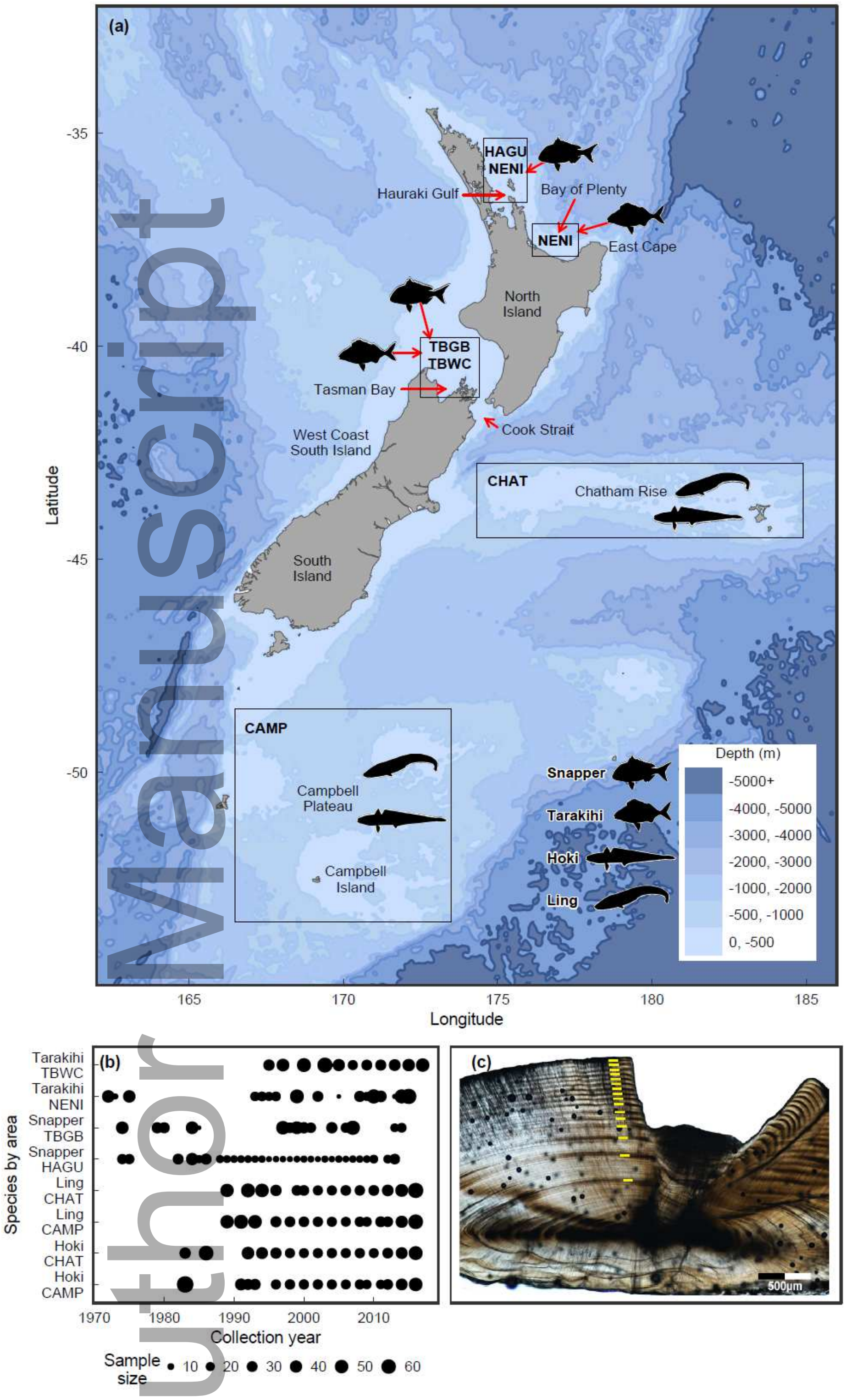

Figure 1: (a) Map of New Zealand showing fish sample locations; (b) graphical summary of otolith samples for each species by area combination used in this study; and (c) transverse section of a 16+ year old snapper's sagital otolith, illustrating growth increments along the primordium to ventro-sulcal ageing axis.

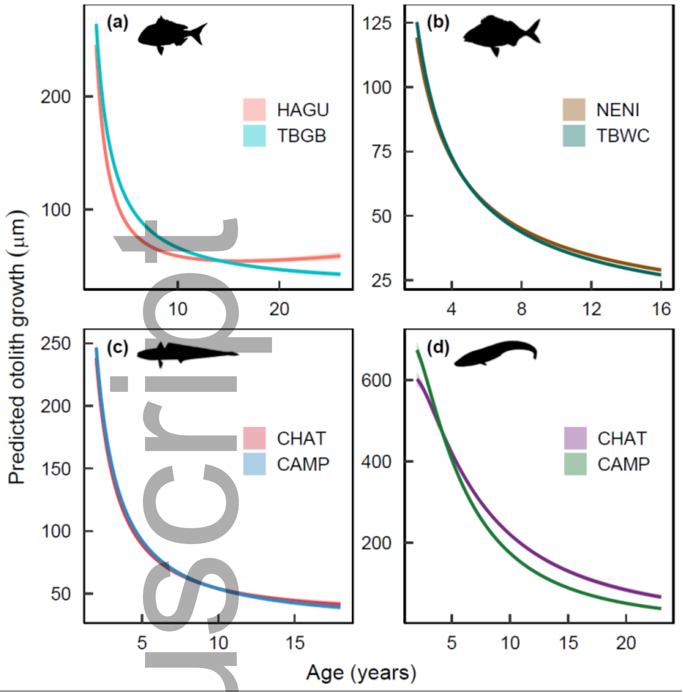

Figure 2: Age-dependent annual otolith growth (μm, ±95% CI) for each sample area in (a) snapper, (b) tarakihi, (c) hoki, and (d) ling.

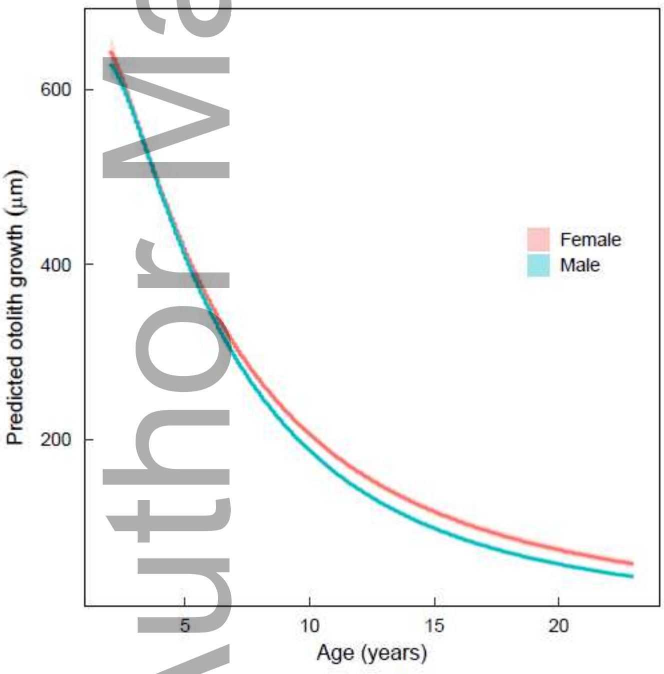

Figure 3: Age-dependent annual otolith growth (μm, ±95% CI) for female and male ling.

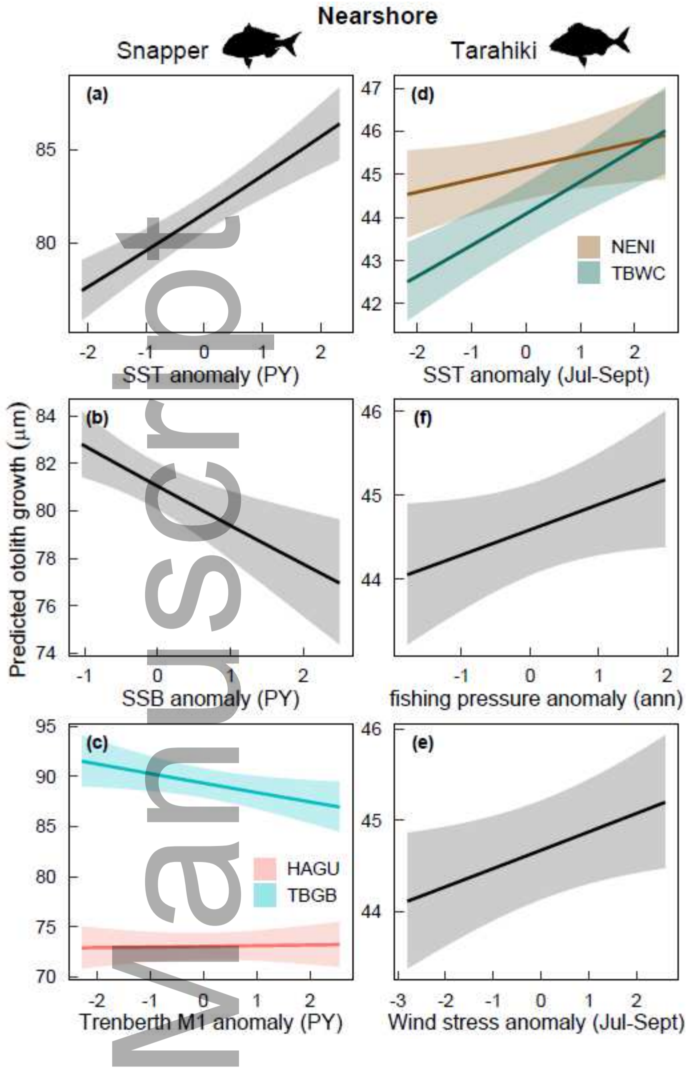

Figure 4: Annual growth variation (µm of otolith growth, ±95% CI) of nearshore species as a function of extrinsic factors. (a) Snapper growth response to the previous year's SST, (b) SSB, and (c) area-specific snapper growth responses to the previous year's meridional winds. (d) Tarakihi area-specific growth response to July–September SST, (e) fishing pressure, and (f) July–September wind stress. PY: previous year; SST: sea surface temperature; SSB: spawning stock biomass.

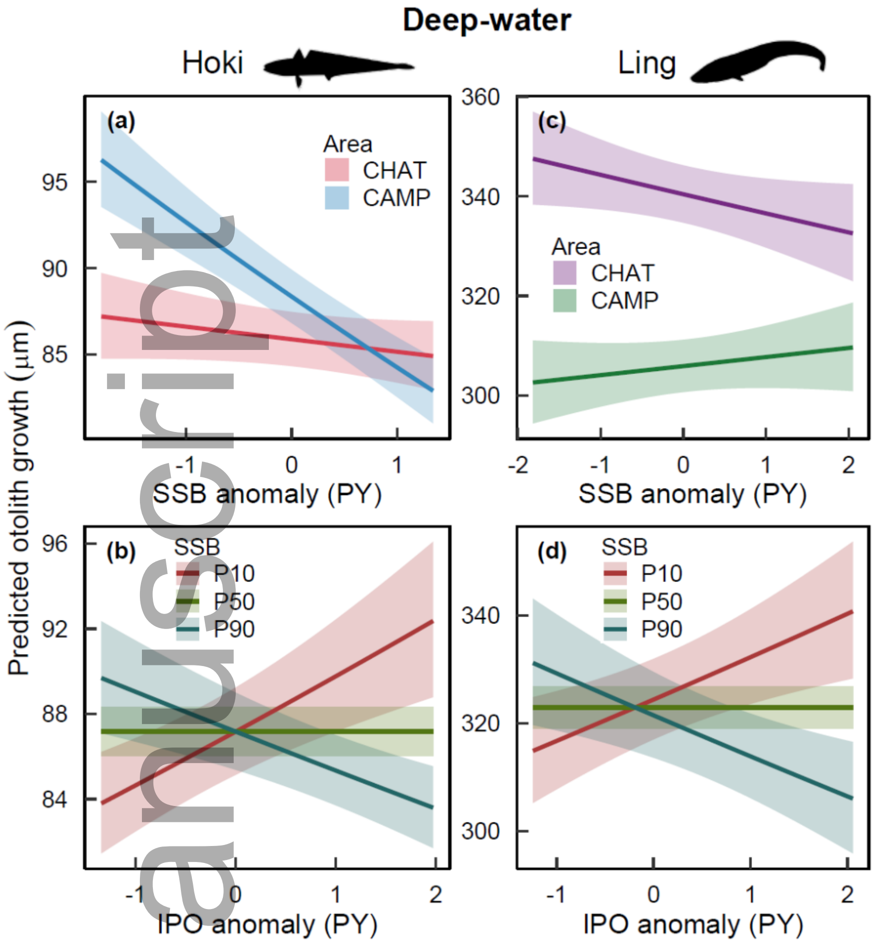

426

427 **Figure 5:** Annual growth variation (µm of otolith growth, ±95% CI) of deep-water species as
428 a function of extrinsic factors. (a) Area-specific hoki growth response to the previous year's
429 SSB, and (b) the interaction between the previous year's SSB and IPO. (c) Area-specific ling
430 growth response to the previous year's SSB, and (d) the interaction between the previous
431 year's SSB and IPO. PY: previous year; SSB: spawning stock biomass; IPO: Interdecadal Pacific
432 Oscillation. Note: P10, P50 and P90 refer to the 10% 50% and 90% percentile value of
433 observed SSB.

434

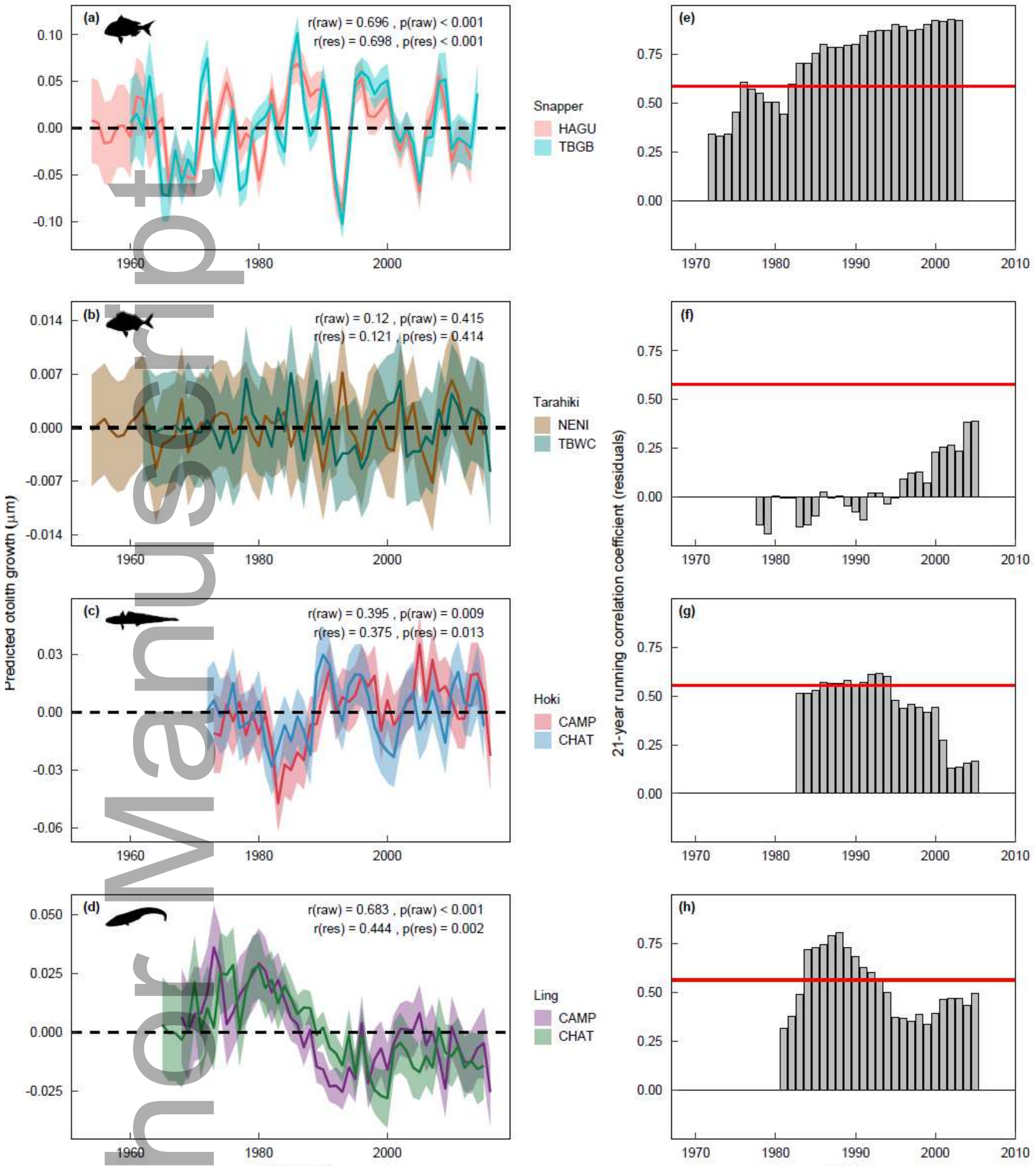

Figure 6: (a–d) Predicted area-specific annual growth biochronologies (μm of otolith growth, ± standard error) with raw and residual (temporal trend and auto-correlation removed; see text) within species zero-lag cross correlations for snapper, tarakihi, hoki, and ling. Dotted horizontal lines represent long-term mean growth for each species (model fixed effect intercept). (e–h) 21-year within-species running correlations of annual growth residuals (see text; bars), plotted on the central year of each window. The red horizontal line represents the threshold above which running correlations are significant at the 0.05 level. Note, each

species' running correlations are based on a subset of years for which annual sample depth was at least five increment measurements (snapper: 1962-2013; tarakihi: 1968-2015; hoki: 1973-2015; ling: 1971-2015).

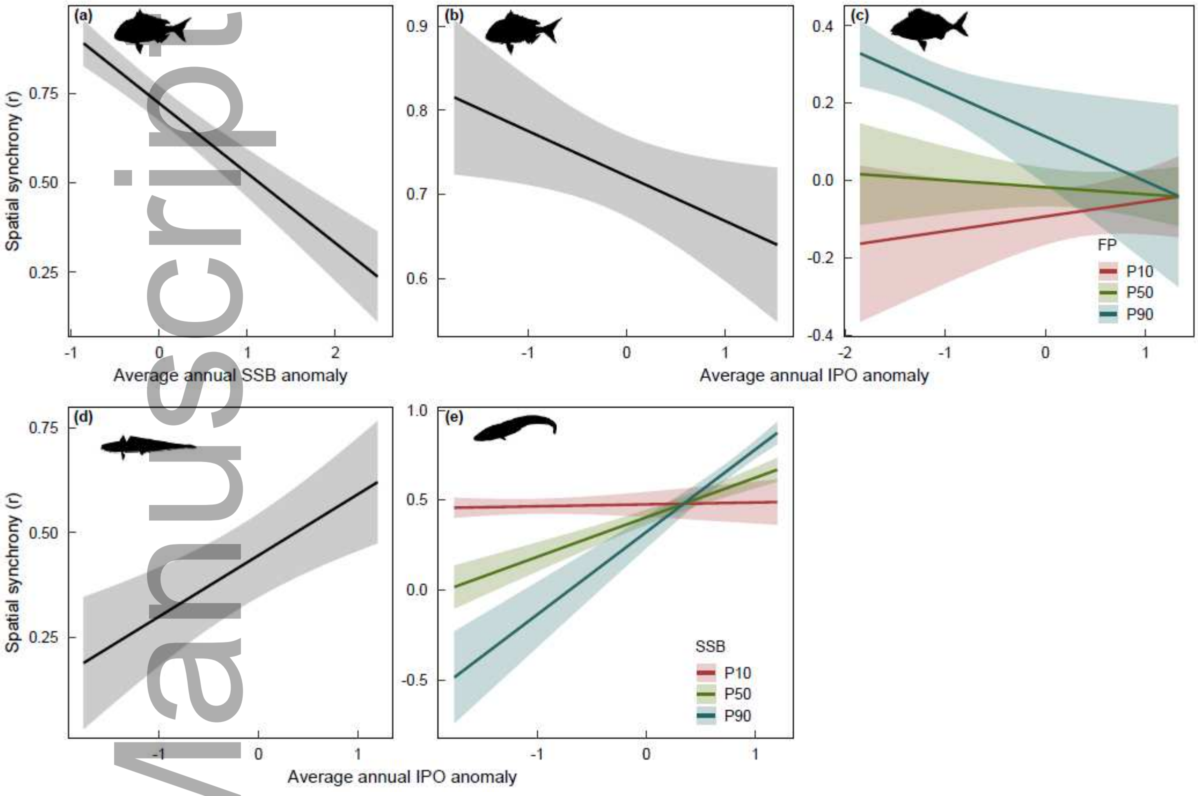

Figure 7: Predicted relationships (±95% CI) between estimates of time-varying spatial synchrony (21-year running correlation r) and 21-year rolling means of annual extrinsic factors. Spatial synchrony responses of: snapper to (a) SSB and (b) IPO; (c) tarakihi to IPO and fishing pressure; (d) hoki to IPO; and (e) ling to IPO and SSB. SSB: spawning stock biomass; IPO: Interdecadal Pacific Oscillation; FP: fishing pressure. Note: P10, P50 and P90 refer to the 10% 50% and 90% percentile value of observed FP and SSB.

Discussion

Natural and anthropogenically driven changes to the marine environment, coupled with harvest-related shifts in population size, additively and synergistically influenced the degree of average individual growth and population-level spatial synchrony across our four study species. Within stocks, surviving individuals have benefited from historical and current fishing practices as it released them from regulating density-dependent processes. Conversely, fishing-induced abundance reductions have increased stock synchrony and thus potentially increased the vulnerability of species to environmental change. The strong environmental signals in our data indicate that individual growth will initially increase in a warmer future and forthcoming positive IPO phase. However, the implications for this change on fishery productivity remain less clear due to the contrasting effects of fishing at the within and among stock scales.

Intrinsic drivers of annual growth

Spatial differences in age-dependent growth are likely to be driven primarily by environmental factors, given the lack of any marked genetic heterogeneity across our putative stocks (Fisheries New Zealand, 2019). Previous work using size-at-age data has identified differences between male and female age-dependent growth for ling and hoki (females attain larger size: Horn, 2005, Horn, 1993, Horn & Sullivan, 1996), but not snapper and tarakihi (Walsh *et al.*, 2016, Walsh *et al.*, 2014). Our increment-based results generally conform with these expectations, although the lack of detectable sex-specific differences in hoki could reflect the relatively small differences in length-at-age (Horn & Sullivan, 1996).

Natural and artificial selection both impact the expression of an individual's average lifetime growth rate. For our inshore species (snapper and tarakihi), individuals caught at younger ages had, on average, grown at a faster rate than fish caught when older. We believe that these patterns are representative of fishing selectivity, whereby faster growing individuals within a cohort become vulnerable to capture at a younger age, or overall increases in mortality risk are selecting for earlier maturation and thus faster growth (Audzijonyte *et al.*, 2016). Conversely, relatively more slow-growing ling were captured at younger ages during the trawl surveys. Such a pattern is suggestive of size selective natural mortality (Sogard, 1997) favouring faster growing individuals to live longer (e.g. Tanner *et al.*, 2019). Regardless of the cause, our modelling approach ensured that we could identify and account for any ecological, evolutionary, or sample regime-dependent biases in annual growth variation (Morrongiello *et al.*, 2012).

Extrinsic drivers of annual growth

The internal body temperature of ectotherms like fish largely depends on environmental temperature. This means that key biological processes such as metabolic rate, digestion rate, muscle activity and reproductive allocation- all linked to somatic growth rate (Audzijonyte *et al.*, 2019)- can be directly regulated by water temperature. Ectotherm growth can also be indirectly affected by temperature, such as when warming causes changes in food quality or quantity or alters interspecific interactions (Behrenfeld *et al.*, 2006, Kordas *et al.*, 2011). Snapper and tarakihi share a similar diet (Table S1; Stevens *et al.*, 2011) and their annual growths were positively related to SST. Tarakihi growth was correlated with winter SST (stronger in the cooler TBWC population) and we believe this is indicative of a direct temperature effect. Whilst empirical studies on tarakihi thermal tolerance have not been performed, inference can be drawn from their spatial distribution (Stuart-Smith *et al.*, 2015). Tarakihi commonly experience annual temperatures ranging from 12.7^{o}C to 20.3^{o}C (10th and 90th percentile; Kaschner *et al.*, 2019). Winter temperatures in our more poleward (TBWC) and equatorial (NENI) populations ranged from 12.6-14.2^{o}C and 14.9-16.8^{o}C respectively. A greater growth response to warming would therefore be expected in TBWC as conditions move toward a thermal optimum whereas NENI fish will be closer to this point already.

Snapper growth was correlated with annual SST from the previous growth year. We interpret this lagged SST response as an indirect effect of warming that promoted the recruitment or survival of snapper food (crabs, shellfish, echinoderms and polychaetes). Such a temperature-induced productivity pulse may take a year to become available to adult snapper (e.g. Frederiksen *et al.*, 2006, Nguyen *et al.*, 2015). Previous work has shown that snapper growth elsewhere in its range is positively related to SST up to an optimal of c. 19–20°C, whereafter growth declines with additional warming (Martino *et al.*, 2019, Wakefield *et al.*, 2016). HAGU snapper and NENI tarakihi populations are already experiencing temperatures close to their potential thermal optimum (annual maximum in our study of 19^{o}C). Depending on the relative importance of direct and indirect mechanisms, projected increases in SST may initially cause an increase in growth for both species in their more equatorial populations, followed by a decline (Morrongiello & Thresher, 2015, Neuheimer *et al.*, 2011). Warming will continue to promote the somatic growth of fish in more poleward, cooler populations.

Wind direction and wind strength play an important role in determining water column mixing, sea surface temperature, and associated rates of primary productivity (e.g. Longdill *et al.*, 2008, Lozier *et al.*, 2011, Schofield *et al.*, 2018). Annual snapper growth was generally higher, especially in the south, following years of weaker meridional (northly) winds. These conditions promote stratification and may lead to warmer, more favourable temperatures for snapper prey (Chang *et al.*, 2003). Tarakihi growth was higher in years where the winter had greater offshore wind stress. Offshore winds aid mixing which promotes primary productivity in New Zealand coastal waters (Longdill *et al.*, 2008), which in turn may support tarakihi food (Stevens *et al.*, 2011). There has been a recent increase in Southern Hemisphere mid latitude westerly winds attributable to climate change (Thompson & Solomon, 2002), and this trend is expected to continue over the next 50 years (Mullan *et al.*, 2001). We speculate that these stronger zonal winds will promote primary productivity in coastal waters (sensu Sydeman *et al.*, 2014) and lead to an increase in snapper and tarakihi growth rates.

The effects of spawning stock biomass and fishing pressure on growth were apparent for all species. The patterns observed were consistent with individual fish growing faster when biomass was lower, suggesting a release from density-dependent growth control (Lorenzen & Enberg, 2002, Morrongiello *et al.*, 2019), and/or reflective of size selective harvest and increased mortality driving the expression of elevated juvenile growth (Audzijonyte *et al.*, 2016). Contrasting spatial differences in the effect of spawning stock biomass were detected for hoki and ling, with the growth of CAMP hoki (larger absolute biomass) and CHAT ling (smaller absolute biomass) more sensitive to changes in this variable. It is likely that relative changes in biomass or habitat alteration associated with trawl fishing, not absolute changes in stock size, drives the observed growth variation. Interestingly, the growth of snapper and tarakihi experienced only additive effects of fishing and environmental variation despite both species being heavily harvested and there being stock-specific differences in fishing pressure (Figure S1; Fisheries New Zealand, 2019). These results suggest that regional environmental variation has always had a strong influence on the productivity of New Zealand's nearshore fish stocks, regardless of whether they are fished or not (e.g. Gillanders *et al.*, 2012).

The growth of deep-water species is often driven by factors and at time scales different to those operating at the surface (Nguyen *et al.*, 2015, Tanner *et al.*, 2020). These differences arise because deep-water environments are relatively constant and the assimilation of surface-derived primary productivity into deep-water food webs takes time (Dickey, 2001, Morales-Nin & Panfili, 2005). The IPO is a complex, multi-decadal and Pacific-wide, climate phenomena. During positive phases of the IPO, the south Pacific convergence zone (SPCZ) shifts southwest and the waters around New Zealand become cooler than average, south-westerly winds become stronger, the weather stormier, and waves bigger (Folland *et al.*, 2002, Godoi *et al.*, 2018, Salinger *et al.*, 2001). These weather conditions can result in deeper mixed layers (Carranza *et al.*, 2018) and potentially a greater subsidy of surface productivity to the deep (Pinkerton *et al.*, 2019). We detected a synergistic effect of lagged IPO and spawning stock biomass on the annual growth of hoki and ling. The importance of lagged IPO could arise if its multi-decadal cycle of influence at the surface (Henley *et al.*, 2015) allows this ocean-wide phenomenon to be more strongly integrated into higher trophic levels of the food web at depth (sensu Di Lorenzo & Ohman, 2013). Positive IPO phases are characterised by favourable environmental conditions for growth, and this benefit is likely maximised when intraspecific competition (related to biomass) is low. Therefore, our results suggest that density dependence can limit the capacity of individuals to respond to favourable conditions. Under current fisheries management practice, future SSB will likely remain around the 40% reference point while IPO is forecast to enter a positive phase (Henley *et al.*, 2017, Meehl *et al.*, 2016). These conditions indicate that hoki and ling annual growth rate will increase over the next decade.

Spatial synchrony in annual growth

Spatial synchrony in populations is widely believed to be driven by three non-exclusive natural processes: rates of individual dispersal, strength of environmental factors, and trophic interactions (Liebhold *et al.*, 2004). The strong link between all four species' spatial synchrony time series and IPO is intuitive given the IPO has a periodicity of 10-30 years (Parker *et al.*, 2007) and our running correlations were calculated over a 21 year window. The increasing spatial synchrony in nearshore species during the recent negative IPO phase could be, in part, related to the associated warming of coastal waters (see above). Conversely, predicted reductions in region-wide surface-to-deep trophic subsidies during the same negative IPO phases may lead to a dominance of local scale processes on growth (e.g. habitat complexity; Brown *et al.*, 2019) and thus the observed reduction in hoki and ling spatial synchrony.

Temporal patterns in the spatial synchrony of our stock somatic growth rates is most likely driven by unifying environmental conditions (i.e. 'Moran Effect'), with this sensitivity further amplified by fishing activity in some species. For tarakihi and ling, increased fishing pressure (and its correlate, reduced spawning stock biomass) amplified the effect of IPO on spatial synchrony. For tarakihi, this occurred despite both stocks experiencing very different fishing mortalities, albeit with a similar trend (Figure S1). Snapper synchrony was affected by fishing in a similar, but solely, additive way. Fishing reduces population density (Lorenzen & Enberg, 2002) and truncates a population's demographic structure (Barnett *et al.*, 2017). Both these fishing-induced mechanisms, reduced density dependence and demographic truncation, can impact on an individual or population's environmental sensitivity and hence its likelihood of spatial synchrony. Less competition for resources can be beneficial and allow surviving individuals to have greater capacity to track favourable conditions (Morrongiello *et al.*, 2019). Conversely, a loss of phenotypic diversity can erode the capacity of populations to buffer against environmental change (Gamelon *et al.*, 2019).

Despite evidence of within-species spatial synchrony in growth, correlations between species in the same location were generally weak. This result contrasts those from a recent study that detected among-species growth synchrony in the deep-water fish from the Azores (Tanner *et al.*, 2020). Our analyses of extrinsic drivers of growth showed strong similarities in the importance of environmental variables for nearshore and deep-water species. It is possible then that different fishing histories have induced varying levels of impact on each species' demographic structure (Fisheries New Zealand, 2019), and in turn reduced apparent among-species spatial synchrony. Previous work has found that dispersal can induce spatial synchrony among fish population abundances over distances commensurate with ecologically relevant dispersal (Cheal *et al.*, 2007). In our case, fish populations were between 400-600nm apart and so we suspect that not enough fish regularly move between populations to homogenise growth.

Conclusions

Overall, environmental change and fishing activity are having an important impact on the growth rate, and thus productivity of four of New Zealand's most important nearshore and deep-water fisheries. Historical and current fishing practices increased stock synchrony

(Moran Effect) and thus potentially the vulnerability of species to environmental change. Conversely, within stocks individuals benefited from fishing as it released them from regulating density-dependent processes. Nearshore species were most strongly linked to regional-scale variables, while deep-water species responded to basin-scale drivers. The functional relationships identified here between environmental parameters and a proxy for somatic growth can be used to increase the reality of future stock assessments. The inclusion of environmentally driven growth patterns could increase the predictive power of models and will also allow for fisheries scenario testing under a range of warming futures.

Acknowledgements

NOAA_ERSST_V5 and NOAA High Resolution SST data were provided by the NOAA/OAR/ESRL PSD, Boulder, Colorado, USA, from their Web site at http://www.esrl.noaa.gov/psd/. MODIS data we accessed from the NASA Goddard Space Flight Center, Ocean Ecology Laboratory, Ocean Biology Processing Group. We thank Thomas Schmitt and Henry Wootton for help producing figures, and Clement Zhong Wang Ng for producing the graphical abstract. This research was funded by a New Zealand Ministry of Business, Innovation and Employment (MBIE) Smart Ideas grant (contract C01X1619) awarded to PLH and JRM. JRM was also partly supported by the Australian Research Council (DP190101627) and the Australian Academy of Science's Thomas Davies Research Grant. The authors declare no conflict of interest.

Data availability statement

[illegible]

[illegible]

⍰⍰⍰ ⍰⍰⍰⍰⍰⍰⍰⍰⍰⍰⍰⍰⍰ ⍰⍰⍰⍰⍰ ⍰⍰⍰⍰⍰ ⍰⍰⍰⍰⍰ ⍰⍰⍰⍰⍰ ⍰⍰⍰⍰⍰⍰⍰⍰⍰ ⍰⍰⍰⍰ ⍰⍰⍰⍰⍰ ⍰⍰⍰⍰⍰⍰ ⍰⍰⍰⍰⍰ ⍰⍰⍰⍰⍰⍰ ⍰⍰⍰⍰⍰⍰⍰⍰⍰

The data that support the findings of this study are openly available in figshare at https://doi.org/10.26188/13377302

References

Anderson CNK, Hsieh C-H, Sandin SA *et al.* (2008) Why fishing magnifies fluctuations in fish abundance. Nature*,* **452**, 835-839.

Anderson O, Bagley N, Hurst R, Francis M, Clark M, McMillan P (1998) Atlas of New Zealand fish and squid distributions from research bottom trawls. pp Page, Wellington, NIWA Technical Report 42. 303 p.

Audzijonyte A, Barneche DR, Baudron AR *et al.* (2019) Is oxygen limitation in warming waters a valid mechanism to explain decreased body sizes in aquatic ectotherms? Global Ecology and Biogeography*,* **28**, 64-77.

Audzijonyte A, Fulton E, Haddon M *et al.* (2016) Trends and management implications of human-influenced life-history changes in marine ectotherms. Fish Fish*,* **17**, 1005-1028.

Barneche DR, Robertson DR, White CR, Marshall DJ (2018) Fish reproductive-energy output increases disproportionately with body size. Science*,* **360**, 642-645.

Barnett LA, Branch TA, Ranasinghe RA, Essington TE (2017) Old-growth fishes become scarce under fishing. Current Biology*,* **27**, 2843-2848. e2842.

Bates D, Mächler M, Bolker B, Walker S (2015) Fitting linear mixed-effects models using lme4. Journal of Statistical Software*,* **67**, 48.

Behrenfeld MJ, O'malley RT, Siegel DA *et al.* (2006) Climate-driven trends in contemporary ocean productivity. Nature*,* **444**, 752-755.

Bergenius MA, Meekan MG, Robertson RD, Mccormick MI (2002) Larval growth predicts the recruitment success of a coral reef fish. Oecologia*,* **131**, 521-525.

Black BA, Allman RJ, Schroeder ID, Schirripa MJ (2011) Multidecadal otolith growth histories for red and gray snapper (Lutjanus spp.) in the northern Gulf of Mexico, USA. Fisheries Oceanography*,* **20**, 347-356.

Bowen M, Markham J, Sutton P, Zhang X, Wu Q, Shears NT, Fernandez D (2017) Interannual variability of sea surface temperature in the southwest Pacific and the role of ocean dynamics. Journal of Climate*,* **30**, 7481-7492.

Brown CJ, Broadley A, Adame MF, Branch TA, Turschwell MP, Connolly RM (2019) The assessment of fishery status depends on fish habitats. Fish and Fisheries*,* **20**, 1-14.

Carranza MM, Gille ST, Franks PJS, Johnson KS, Pinkel R, Girton JB (2018) When mixed layers are not mixed. Storm-driven mixing and bio-optical vertical gradients in mixed layers of the southern ocean. Journal of Geophysical Research: Oceans*,* **123**, 7264-7289.

Carton JA, Chepurin GA, Chen L (2018) SODA3: A new ocean climate reanalysis. Journal of Climate*,* **31**, 6967-6983.

Chang FH, Zeldis J, Gall M, Hall J (2003) Seasonal and spatial variation of phytoplankton assemblages, biomass and cell size from spring to summer across the north-eastern New Zealand continental shelf. Journal of Plankton Research*,* **25**, 737-758.

Cheal AJ, Delean S, Sweatman H, Thompson AA (2007) Spatial synchrony in coral reef fish populations and the influence of climate. Ecology*,* **88**, 158-169.

Cheng L, Abraham J, Hausfather Z, Trenberth KE (2019) How fast are the oceans warming? Science*,* **363**, 128-129.

Ciannelli L, Chan K-S, Bailey KM, Stenseth NC (2004) Nonadditive effects of the environment on the survival of a large marine fish population. Ecology*,* **85**, 3418-3427.

Di Lorenzo E, Ohman MD (2013) A double-integration hypothesis to explain ocean ecosystem response to climate forcing. Proceedings of the National Academy of Sciences*,* **110**, 2496-2499.

Dickey TD (2001) The role of new technology in advancing ocean biogeochemical research. Oceanography*,* **14**, 108-120.

Enberg K, Jorgensen C, Dunlop ES *et al.* (2012) Fishing-induced evolution of growth: concepts, mechanisms and the empirical evidence. Marine Ecology*,* **33**, 1-25.

Engen S, Cao FJ, Sæther B-E (2018) The effect of harvesting on the spatial synchrony of population fluctuations. Theoretical Population Biology*,* **123**, 28-34.

Fisheries New Zealand (2019) Fisheries assessment plenary, May 2019: stock assessments and stock status. Compiled by the Fisheries Science and Information Group, Fisheries New Zealand, Wellington, New Zealand. 1637 pp. pp Page.

Folland CK, Renwick JA, Salinger MJ, Mullan AB (2002) Relative influences of the Interdecadal Pacific Oscillation and ENSO on the South Pacific Convergence Zone. Geophysical Research Letters*,* **29**, 21-21.

Fox J, Weisberg S (2019) *An R Companion to Applied Regression, 3rd Edition,* Thousand Oaks, CA, Sage publications.

Frank KT, Petrie B, Leggett WC, Boyce DG (2016) Large scale, synchronous variability of marine fish populations driven by commercial exploitation. Proceedings of the National Academy of Sciences*,* **113**, 8248-8253.

Frederiksen M, Edwards M, Richardson AJ, Halliday NC, Wanless S (2006) From plankton to top predators: bottom-up control of a marine food web across four trophic levels. Journal of Animal Ecology*,* **75**, 1259-1268.

Gamelon M, Sandercock BK, Sæther B-E (2019) Does harvesting amplify environmentally induced population fluctuations over time in marine and terrestrial species? Journal of Applied Ecology, **56**, 2186-2194.

Gelman A, Su Y-S (2020) arm: data analysis using regression and multilevel/hierarchical models. R package version 1.11-2. https://CRAN.R-project.org/package=arm.

Gillanders B, Black B, Meekan M, Morrison M (2012) Climatic effects on the growth of a temperate reef fish from the Southern Hemisphere: a biochronological approach. Marine biology, **159**, 1327-1333.

Godoi VA, Bryan KR, Gorman RM (2018) Storm wave clustering around New Zealand and its connection to climatic patterns. International Journal of Climatology, **38**, e401-e417.

Hannah J, Bell RG (2012) Regional sea level trends in New Zealand. Journal of Geophysical Research: Oceans, **117**.

Hare SR, Mantua NJ (2000) Empirical evidence for North Pacific regime shifts in 1977 and 1989. Progress in Oceanography, **47**, 103-145.

Heino M, Kaitala V, Ranta E, Lindström J (1997) Synchronous dynamics and rates of extinction in spatially structured populations. Proceedings of the Royal Society of London. Series B: Biological Sciences, **264**, 481-486.

Henley BJ, Gergis J, Karoly DJ, Power S, Kennedy J, Folland CK (2015) A tripole index for the interdecadal Pacific oscillation. Climate Dynamics, **45**, 3077-3090.

Henley BJ, Meehl G, Power SB *et al.* (2017) Spatial and temporal agreement in climate model simulations of the Interdecadal Pacific Oscillation. Environmental Research Letters, **12**, 044011.

Hilborn R, Amoroso RO, Anderson CM *et al.* (2020) Effective fisheries management instrumental in improving fish stock status. Proceedings of the National Academy of Sciences, **117**, 2218-2224.

Horn P (2005) A review of the stock structure of ling (*Genypterus blacodes*) in New Zealand waters. In: *New Zealand Fisheries Assessment Report 2005/59. 41 p.* pp Page.

Horn PL (1993) Growth, age structure, and productivity of ling, Genypterus blacodes (Ophidiidae), in New Zealand waters. New Zealand Journal of Marine and Freshwater Research, **27**, 385-397.

Horn PL, Sullivan KJ (1996) Validated aging methodology using otoliths, and growth parameters for hoki (*Macruronus novaezelandiae*) in New Zealand waters. New Zealand Journal of Marine and Freshwater Research, **30**, 161-174.

Huang B, Thorne PW, Banzon VF *et al.* (2017) Extended reconstructed sea surface temperature, version 5 (ERSSTv5): upgrades, validations, and intercomparisons. Journal of Climate*,* **30**, 8179-8205.

Jenkins GP (2005) The influence of climate on the fishery recruitment of a temperate, seagrass-associated fish, the King George whiting *Sillaginodes punctata*. Marine Ecology Progress Series*,* **288**, 263-271.

Kaschner K, Kesner-Reyes K, Garilao C, Rius-Barile J, Rees T, Froese R (2019) AquaMaps: Predicted range maps for aquatic species. World wide web electronic publication, www.aquamaps.org, version 10/2019 (preliminary). pp Page.

Kjesbu OS, Bogstad B, Devine JA *et al.* (2014) Synergies between climate and management for Atlantic cod fisheries at high latitudes. Proceedings of the National Academy of Sciences*,* **111**, 3478-3483.

Kobayashi S, Ota Y, Harada Y *et al.* (2015) The JRA-55 reanalysis: General specifications and basic characteristics. Journal of the Meteorological Society of Japan. Ser. II*,* **93**, 5-48.

Kordas RL, Harley CDG, O'Connor MI (2011) Community ecology in a warming world: The influence of temperature on interspecific interactions in marine systems. Journal of Experimental Marine Biology and Ecology*,* **400**, 218-226.

Le Bris A, Mills KE, Wahle RA *et al.* (2018) Climate vulnerability and resilience in the most valuable North American fishery. Proceedings of the National Academy of Sciences*,* **115**, 1831-1836.

Liebhold A, W.D. K, Bjørnstad ON (2004) Spatial synchrony in population dynamics. Annual Review of Ecology, Evolution, and Systematics*,* **35**, 467-490.

Lobón-Cerviá J (2009) Why, when and how do fish populations decline, collapse and recover? The example of brown trout (*Salmo trutta*) in Rio Chaballos (northwestern Spain). Freshwater Biology*,* **54**, 1149-1162.

Longdill PC, Healy TR, Black KP (2008) Transient wind-driven coastal upwelling on a shelf with varying width and orientation. New Zealand Journal of Marine and Freshwater Research*,* **42**, 181-196.

Lorenzen K, Enberg K (2002) Density-dependent growth as a key mechanism in the regulation of fish populations: evidence from among-population comparisons. Proceedings of the Royal Society B-Biological Sciences*,* **269**, 49-54.

Lozier MS, Dave AC, Palter JB, Gerber LM, Barber RT (2011) On the relationship between stratification and primary productivity in the North Atlantic. Geophysical Research Letters*,* **38**.

Martino JC, Fowler AJ, Doubleday ZA, Grammer GL, Gillanders BM (2019) Using otolith chronologies to understand long-term trends and extrinsic drivers of growth in fisheries. Ecosphere*,* **10**, e02553.

Meehl GA, Hu A, Teng H (2016) Initialized decadal prediction for transition to positive phase of the Interdecadal Pacific Oscillation. Nature Communications*,* **7**, 11718.

Morales-Nin B, Panfili J (2005) Seasonality in the deep sea and tropics revisited: what can otoliths tell us? Marine and Freshwater Research*,* **56**, 585-598.

Morrongiello JR, Sweetman P, Thresher RE (2019) Fishing constrains phenotypic responses of marine fish to climate variability. Journal of Animal Ecology*,* **88**, 1645-1656.

Morrongiello JR, Thresher RE (2015) A statistical framework to explore ontogenetic growth variation among individuals and populations: a marine fish example. Ecological Monographs*,* **85**, 93-115.

Morrongiello JR, Thresher RE, Smith DC (2012) Aquatic biochronologies and climate change. Nat. Clim. Change*,* **2**, 849-857.

Mullan AB, Wratt DS, Renwick JA (2001) Transient model scenarios of climate changes for New Zealand. Weather and Climate*,* **21**, 3-33.

Neuheimer AB, Thresher RE, Lyle JM, Semmens JM (2011) Tolerance limit for fish growth exceeded by warming waters. Nature Climate Change*,* **1**, 110-113.

Nguyen HM, Rountrey AN, Meeuwig JJ *et al.* (2015) Growth of a deep-water, predatory fish is influenced by the productivity of a boundary current system. Scientific Reports*,* **5**, 9044.

Ong JJ, Rountrey AN, Black BA *et al.* (2018) A boundary current drives synchronous growth of marine fishes across tropical and temperate latitudes. Global Change Biology*,* **24**, 1894-1903.

Parker D, Folland C, Scaife A, Knight J, Colman A, Baines P, Dong B (2007) Decadal to multidecadal variability and the climate change background. Journal of Geophysical Research: Atmospheres*,* **112**.

Perry RI, Cury P, Brander K, Jennings S, Mollmann C, Planque B (2010) Sensitivity of marine systems to climate and fishing: Concepts, issues and management responses. J Marine Syst*,* **79**, 427-435.

Pinkerton MH, Sutton PJH, Wood S (2019) Satellite indicators of phytoplankton and ocean surface temperature for New Zealand. NIWA Client Report 2018180WNrev1. Prepared for the Ministry for the Environment. Wellington, New Zealand. pp Page.

Planque B, Fromentin JM, Cury P, Drinkwater KF, Jennings S, Perry RI, Kifani S (2010) How does fishing alter marine populations and ecosystems sensitivity to climate? J Marine Syst*,* **79**, 403-417.

Reynolds RW, Smith TM, Liu C, Chelton DB, Casey KS, Schlax MG (2007) Daily high-resolution-blended analyses for sea surface temperature. Journal of Climate*,* **20**, 5473-5496.

Rogers LA, Dougherty AB (2019) Effects of climate and demography on reproductive phenology of a harvested marine fish population. Global Change Biology*,* **25**, 708-720.

Rouyer T, Ottersen G, Durant JM *et al.* (2011) Shifting dynamic forces in fish stock fluctuations triggered by age truncation? Global Change Biology*,* **17**, 3046-3057.

Rouyer T, Sadykov A, Ohlberger J, Stenseth NC (2012) Does increasing mortality change the response of fish populations to environmental fluctuations? Ecology Letters*,* **15**, 658-665.

Salinger MJ, Basher R, Fitzharris B, Hay J, Jones P, Macveigh J, Schmidely-Leleu I (1995) Climate trends in the South-west Pacific. International Journal of Climatology*,* **15**, 285-302.

Salinger MJ, Renwick JA, Mullan AB (2001) Interdecadal Pacific Oscillation and South Pacific climate. International Journal of Climatology*,* **21**, 1705-1721.

Schindler DE, Hilborn R, Chasco B, Boatright CP, Quinn TP, Rogers LA, Webster MS (2010) Population diversity and the portfolio effect in an exploited species. Nature*,* **465**, 609-612.

Schofield O, Brown M, Kohut J, Nardelli S, Saba G, Waite N, Ducklow H (2018) Changes in the upper ocean mixed layer and phytoplankton productivity along the West Antarctic Peninsula. Philosophical Transactions of the Royal Society A: Mathematical, Physical and Engineering Sciences*,* **376**, 20170173.

Sogard SM (1997) Size-selective mortality in the juvenile stage of teleost fishes: a review. Bulletin of Marine Science*,* **60**, 1129-1157.

Stawitz CC, Essington TE (2019) Somatic growth contributes to population variation in marine fishes. Journal of Animal Ecology*,* **88**, 315-329.

Stevens DW, Hurst RJ, Bagley NW (2011) Feeding habits of New Zealand fishes: a literature review and summary of research trawl database records 1960 to 2000. In: *New Zealand Aquatic Environment and Biodiversity Report No. 85. 213 p.* pp Page, Ministry of Fisheries.

Stuart-Smith RD, Edgar GJ, Barrett NS, Kininmonth SJ, Bates AE (2015) Thermal biases and vulnerability to warming in the world’s marine fauna. Nature*,* **528**, 88.

Sutton PJ, Roemmich D (2001) Ocean temperature climate off north-east New Zealand. New Zealand Journal of Marine and Freshwater Research*,* **35**, 553-565.

Sutton PJH, Bowen M (2019) Ocean temperature change around New Zealand over the last 36 years. New Zealand Journal of Marine and Freshwater Research*,* **53**, 305-326.

Sutton PJH, Bowen M, Roemmich D (2005) Decadal temperature changes in the Tasman Sea. New Zealand Journal of Marine and Freshwater Research*,* **39**, 1321-1329.

Sydeman W, García-Reyes M, Schoeman D, Rykaczewski R, Thompson S, Black BA, Bograd S (2014) Climate change and wind intensification in coastal upwelling ecosystems. Science*,* **345**, 77-80.

Tanner SE, Giacomello E, Menezes GM *et al.* (2020) Marine regime shifts impact synchrony of deep-sea fish growth in the northeast Atlantic. Oikos*,* **n/a**.

Tanner SE, Vieira AR, Vasconcelos RP, Dores S, Azevedo M, Cabral HN, Morrongiello JR (2019) Regional climate, primary productivity and fish biomass drive growth variation and population resilience in a small pelagic fish. Ecological Indicators*,* **103**, 530-541.

Trenberth KE (1976) Fluctuations and trends in indices of the southern hemispheric circulation. Quarterly Journal of the Royal Meteorological Society*,* **102**, 65-75.

Trippel EA (1995) Age at maturity as a stress indicator in fisheries. Bioscience*,* **45**, 759-771.

Uusi-Heikkilä S, Whiteley AR, Kuparinen A *et al.* (2015) The evolutionary legacy of size-selective harvesting extends from genes to populations. Evolutionary Applications*,* **8**, 597-620.

Wakefield CB, Potter IC, Hall NG, Lenanton RC, Hesp SA, Bartolino HEV (2016) Timing of growth zone formations in otoliths of the snapper, Chrysophrys auratus, in subtropical and temperate waters differ and growth follows a parabolic relationship with latitude. Ices Journal of Marine Science*,* **74**, 180-192.

Walsh C, Horn P, McKenzie J, Maolagáin C, Buckthought D, Stevenson M, Sutton C (2016) Age determination protocol for tarakihi (*Nemadactylus macropterus*). In: *New Zealand Fisheries Assessment Report 2016/13. 37 p.* pp Page.

Walsh C, Horn P, McKenzie J, Ó Maolagáin C, Buckthought D, Sutton C, Armiger H (2014) Age determination protocol for snapper (*Pagrus auratus*). In: *New Zealand Fisheries Assessment Report 2014/51. 33 p.* pp Page.

Warnes GR, Bolker B, Lumley T (2020) gtools: various R programming tools. R package version 3.8.2. https://CRAN.R-project.org/package=gtools.

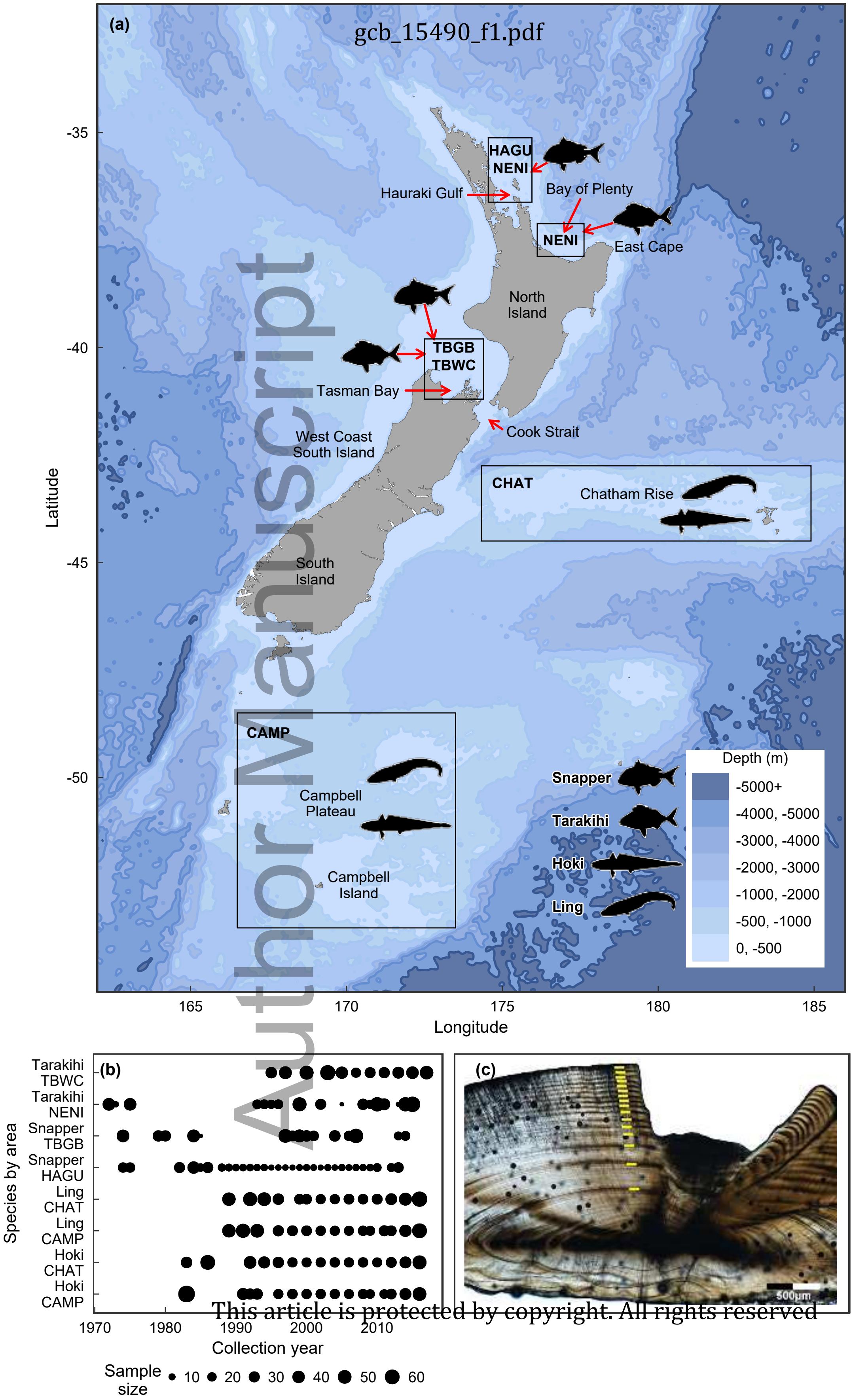
(a)
HAGU
NENI
Hauraki Gulf
Bay of Plenty
NENI
East Cape
North Island
TBGB
TBWC
Tasman Bay
Cook Strait
West Coast South Island
CHAT
Chatham Rise
South Island
CAMP
Campbell Plateau
Campbell Island
Snapper
Tarakihi
Hoki
Ling
Depth (m)
-5000+
-4000, -5000
-3000, -4000
-2000, -3000
-1000, -2000
-500, -1000
0, -500
-35
-40
-45
-50
Latitude
165
170
175
180
185
Longitude
(b)
Tarakihi TBWC
Tarakihi NENI
Snapper TBGB
Snapper HAGU
Ling CHAT
Ling CAMP
Hoki CHAT
Hoki CAMP
Species by area
1970
1980
1990
2000
2010
Collection year
Sample size
10
20
30
40
50
60
(c)
500µm

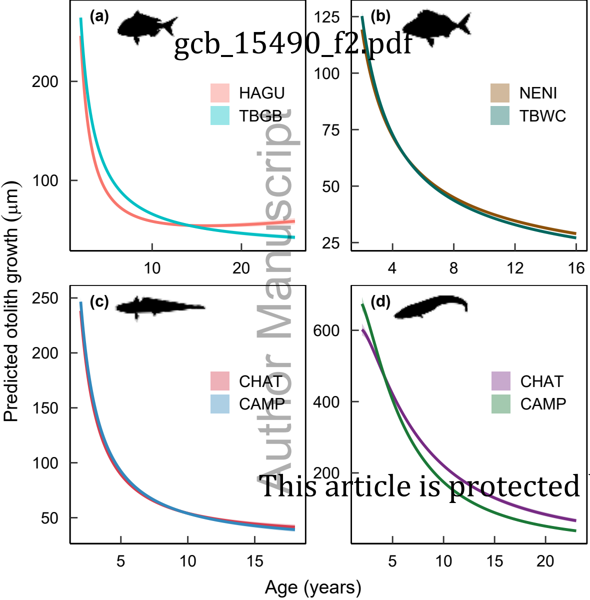
(a)
HAGU
TBGB
200
100
10
20
(b)
NENI
TBWC
125
100
75
50
25
4
8
12
16
(c)
CHAT
CAMP
250
200
150
100
50
5
10
15
(d)
CHAT
CAMP
600
400
200
5
10
15
20
Predicted otolith growth (μm)
Age (years)

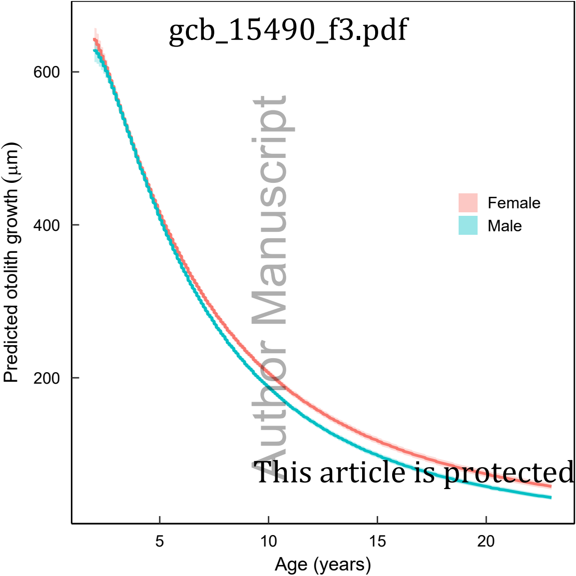
Predicted otolith growth (μm)
600
400
200
5
10
15
20
Age (years)
Female
Male

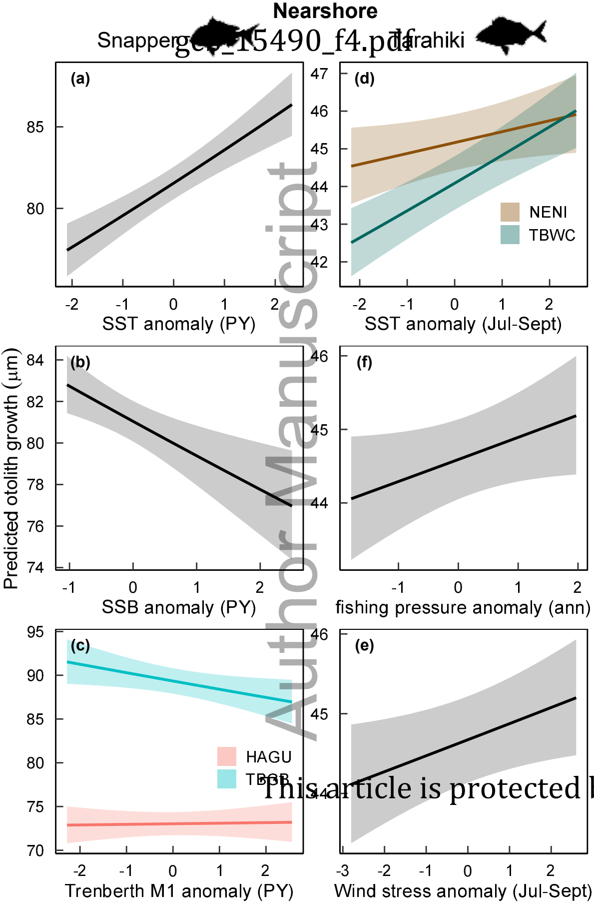
Nearshore
Snapper
Tarakihi
(a)
85
80
-2
-1
0
1
2
SST anomaly (PY)
(d)
47
46
45
44
43
42
NENI
TBWC
-2
-1
0
1
2
SST anomaly (Jul-Sept)
Predicted otolith growth (µm)
(b)
84
82
80
78
76
74
-1
0
1
2
SSB anomaly (PY)
(f)
46
45
44
-1
0
1
2
fishing pressure anomaly (ann)
(c)
95
90
85
80
75
70
HAGU
TBGB
-2
-1
0
1
2
Trenberth M1 anomaly (PY)
(e)
46
45
44
-3
-2
-1
0
1
2
Wind stress anomaly (Jul-Sept)

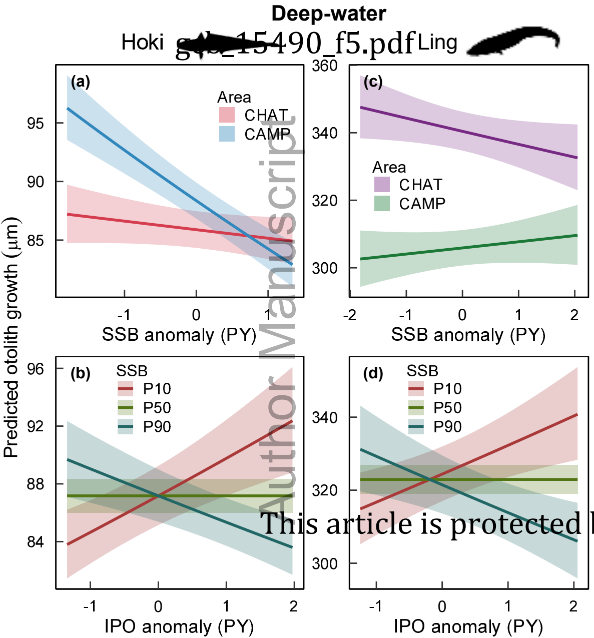
Deep-water
Hoki
Ling
(a)
Area
CHAT
CAMP
95
90
85
-1
0
1
SSB anomaly (PY)
Predicted otolith growth (μm)
(c)
360
340
320
300
Area
CHAT
CAMP
-2
-1
0
1
2
SSB anomaly (PY)
(b)
SSB
P10
P50
P90
96
92
88
84
-1
0
1
2
IPO anomaly (PY)
(d)
SSB
P10
P50
P90
340
320
300
-1
0
1
2
IPO anomaly (PY)

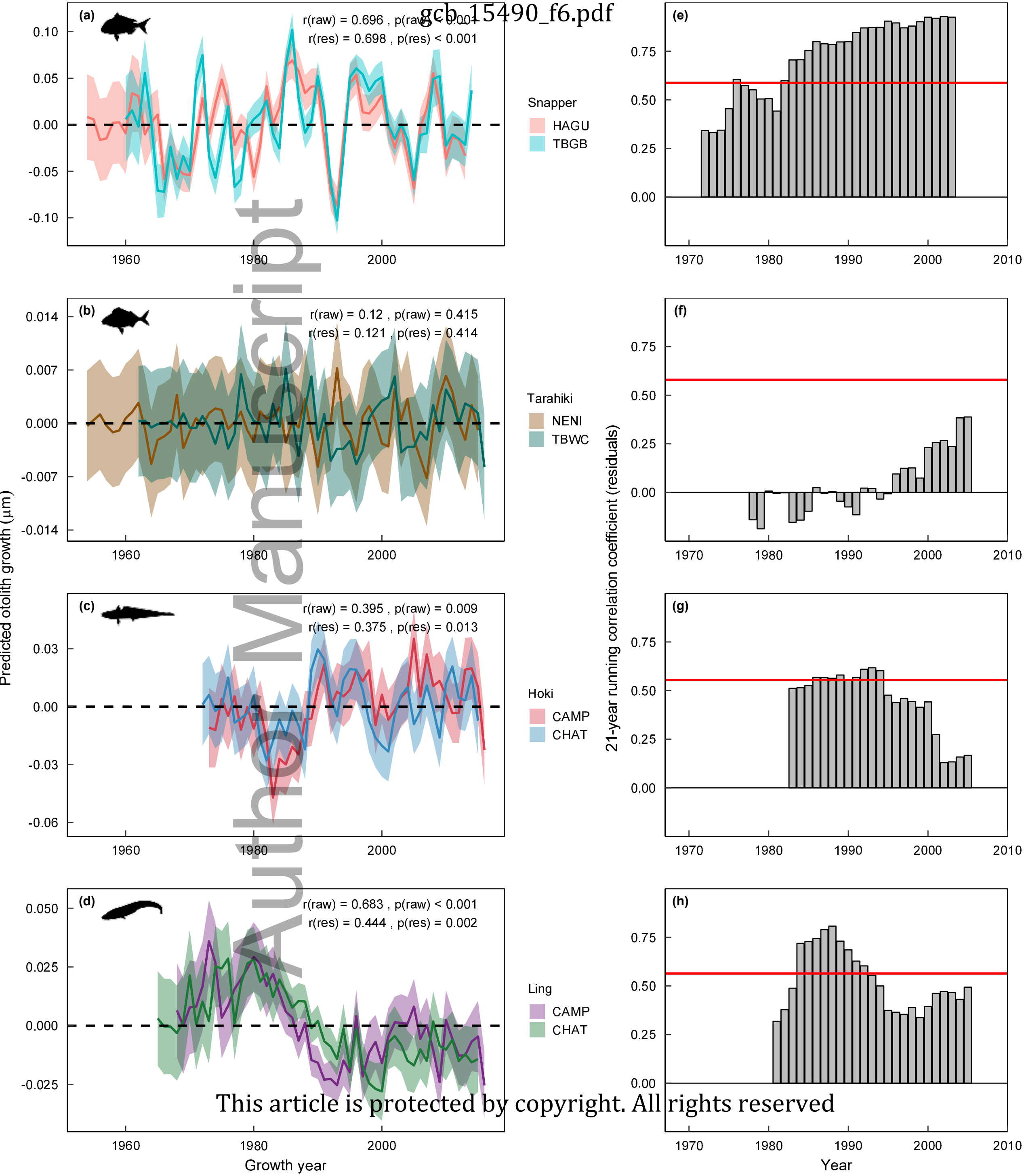
(a)
r(raw) = 0.696 , p(raw) < 0.001
r(res) = 0.698 , p(res) < 0.001
Snapper
HAGU
TBGB
0.10
0.05
0.00
-0.05
-0.10
(b)
r(raw) = 0.12 , p(raw) = 0.415
r(res) = 0.121 , p(res) = 0.414
Tarahiki
NENI
TBWC
0.014
0.007
0.000
-0.007
-0.014
(c)
r(raw) = 0.395 , p(raw) = 0.009
r(res) = 0.375 , p(res) = 0.013
Hoki
CAMP
CHAT
0.03
0.00
-0.03
-0.06
(d)
r(raw) = 0.683 , p(raw) < 0.001
r(res) = 0.444 , p(res) = 0.002
Ling
CAMP
CHAT
0.050
0.025
0.000
-0.025
1960
1980
2000
Growth year
Predicted otolith growth (μm)
(e)
(f)
(g)
(h)
0.75
0.50
0.25
0.00
1970
1980
1990
2000
2010
Year
21-year running correlation coefficient (residuals)

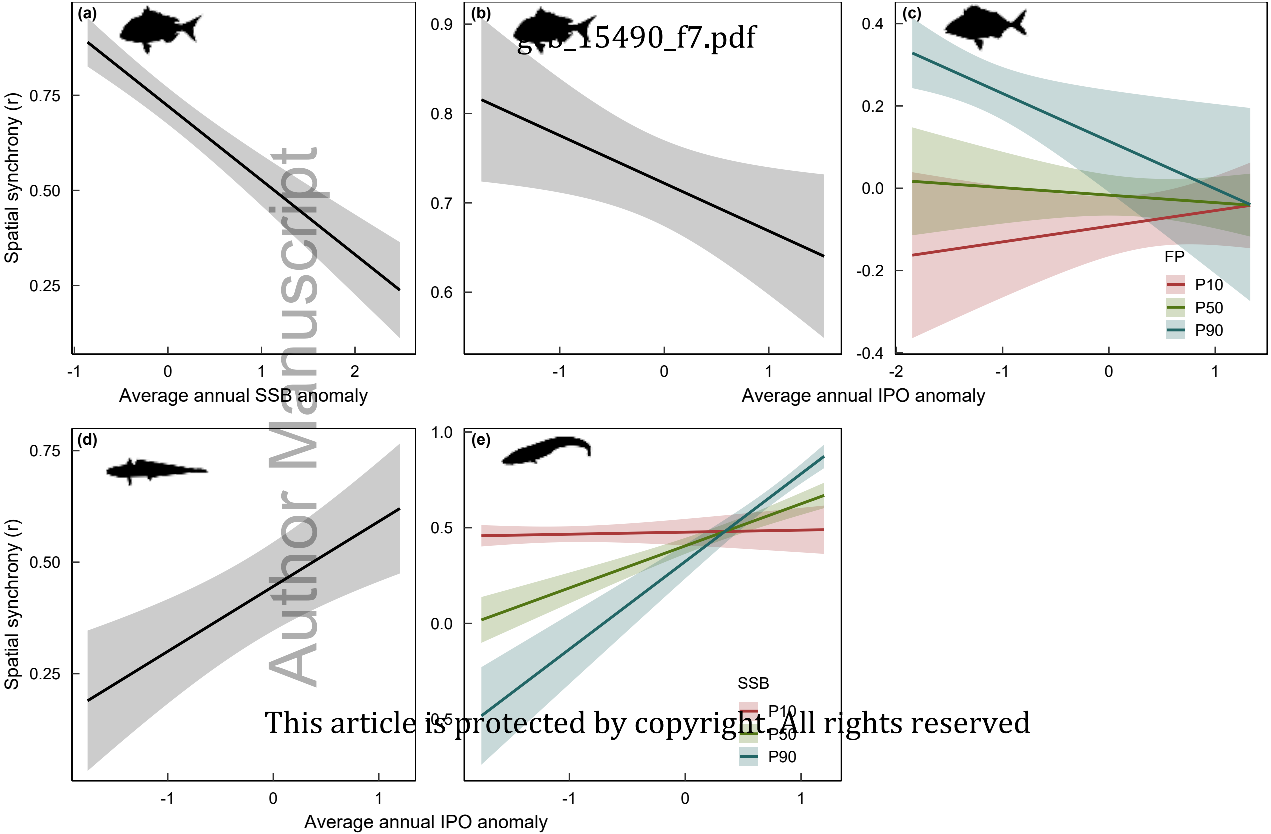
(a)
(b)
(c)
(d)
(e)
Spatial synchrony (r)
0.75
0.50
0.25
-1
0
1
2
Average annual SSB anomaly
0.9
0.8
0.7
0.6
-1
0
1
0.4
0.2
0.0
-0.2
-0.4
-2
-1
0
1
FP
P10
P50
P90
Average annual IPO anomaly
Spatial synchrony (r)
0.75
0.50
0.25
-1
0
1
Average annual IPO anomaly
1.0
0.5
0.0
-0.5
-1
0
1
SSB
P10
P50
P90